Hydrol. Earth Syst. Sci. Discuss., https://doi.org/10.5194/hess-2017-617
Manuscript under review for journal Hydrol. Earth Syst. Sci.
Discussion started: 7 November 2017

Hydrochemical and isotopic evidences for deciphering conceptual model of groundwater salinization processes in a coastal plain, north China

Han Dongmei[a,b]

a Key Laboratory of Water Cycle & Related Land Surface Processes, Institute of Geographic Sciences and Natural Resources Research, Chinese Academy of Sciences, Beijing, 100101, China

b College of Resources and Environment, University of Chinese Academy of Sciences, Beijing 100049, China

Abstract

Groundwater is the important water resource for agricultural irrigation, urban and tourism development and industrial utilization in the coastal region of north China. In the past five decades, coastal groundwater salinization in the Yang-Dai River coastal plain has become more serious than ever before under natural climate change and anthropogenic activities. It is pivotal for the scientific management of coastal water resources to accurately understand groundwater salinization processes and its inducement. Hydrochemical and stable isotopic ($\delta^{18}O$ and $\delta^{2}H$) analysis for the different water bodies (surface water, groundwater, geothermal water, and seawater) were applied to provide a better understanding of the processes of groundwater salinization in the Quaternary aquifers. Saltwater intrusion is the major aspect and can be caused by vertical infiltration along the riverbed at the downstream areas of rivers during the tide/surge period, and lateral inflow into fresh aquifer derived from intensively pumping groundwater. Seawater proportion can reach ~13% in the well field. High mineralized geothermal water (TDS up to 10.6 g/L) with the indicator of paleoseawater relics (lower Cl/Br ratios relative to modern seawater) overflows into the cold Quaternary aquifers. Groundwater salinization can also be exacerbated by the anthropogenic activities (e.g., irrigation return-flow with solution of fertilizers, domestic wastewater discharge). Additionally, the interaction between surface water and groundwater can make the groundwater freshening or salinizing in different sections to locally modify the groundwater hydrochemistry. The cease of the well field and establishment of anti-tide dam in the Yang River estuary area have effective function to contain the development of saltwater intrusion. This study can guide the future water management practices, and provide research approaches and foundation for further investigation of seawater intrusion in this and similar region.

1. Introduction

Coastal region is the key area for the world social and economic development. Approximately 40% of the world's population lives within 100 kilometers of the coast (UN Atlas, 2010). The worldwide coastal area has become increasingly urbanized with 14 of the world's 17 largest cities located along coasts (Creel L., 2003). China has 18,000 km of continental coastline, about 164 million people (about 12% of total Chinese population) live in 14 coastal provinces, and nearly 80% of them distribute in the three coastal economic regions, namely Beijing-Tianjin-Hebei economic region, the Yangtze River delta economic region and the Pearl River delta economic region (Shi, 2012). The rapid economic development and the growing population in the coastal region have increased demands for fresh water, meanwhile been confronted with the threat from waste and sewage water discharge into coastal ecosystems.

Coastal groundwater resources play crucial roles on the social economic and ecologic function in the global coast system (IPCC, 2007). Coastal groundwater system connects the ocean and the continental hydro-ecological systems (Moore, 1996; Ferguson and Gleeson, 2012). Groundwater as an important freshwater resource could be over extracted due to that the periods of highest demand (e.g., agricultural irrigation and tourist seasons) are often the periods of lowest recharge rates (Post, 2005). In addition to occurrence of some environmental issues, such as land subsidence, contaminants transport, the over-exploitation of groundwater can readily result in seawater intrusion in the coastal area. Seawater intrusion has become a global issue and the related studies can be found from the coastal aquifer system of different countries, such as Israel (Sivan et al., 2005;Yechieli et al., 2009; Mazi et al., 2014), Spain (Price and Herman, 1991; Pulido-Leboeuf, 2004; Garing et al., 2013), France (Barbecot et al., 2000; de Montety et al., 2008), Italy (Giambastiani et al.., 2007; Ghiglieri et al., 2012), Morocco (Bouchaou et al., 2008; El Yaouti et al., 2009), USA (Gingerich and Voss, 2002; Masterson, 2004; Langevin et al., 2010), Australia (Zhang et al., 2004; Narayan et al., 2007; Werner, 2010), China (Xue et al.., 2000; Han et al., 2011, 2015), Vietnam (An et al., 2014), Indonesia (Rahmawati et al., 2013), India (Radhakrishna, 2001; Bobba, 2002), Brazil (Gico Montenegro et al., 2006; Cary et al., 2015), etc. Werner et al. (2013) gave an excellent review on seawater intrusion processes, investigation and management. A variety of approaches have been used to investigate seawater intrusion, including head measurement, geophysical methods, geochemical methods (environmental tracers combined hydrochemical and isotope data), conceptual and mathematical modeling (see reviews by Jones et al., 1999; Werner et al., 2013).

Seawater/saltwater intrusion is a complicated hydrogeological process due to the impact of aquifer properties, anthropogenic activities (e.g., intensive groundwater pumping, irrigation practices), recharge rate, variable density flow between the estuary and adjacent fresh groundwater system, tidal/surge activity and global climate change (Ghassemi et al., 1993; Robinson et al., 1998; Smith and Turner, 2001; Simpson and Clement, 2004; Narayan et al., 2007; Werner and Simmons, 2009; Wang et al., 2015). Brockway et al. (2006) reported the negative relationship between saltwater intrusion length and river discharge. Understanding the complex interactions between groundwater and surface water, groundwater and seawater is essential for the effective management of water resources (Sophocleus, 2002; Mondal et al., 2010). There was a vastly different result based on numerical simulations for the additional distance of intrusion in the Nile Delta Aquifer of Egypt and in the Bay of Bengal under the same sea level rise (Sherif and Singh, 1999). Bobba (2002) also employed numerical simulations to demonstrate an apparent risk of saltwater intrusion in the Godavari delta, India due to sea level rise. Westbrook et al. (2005) defined the hyporheic transition zone of mixing between river water and groundwater influenced by tidal fluctuations and the contaminant distribution. Modelling seawater intrusion in the Burdekin Delta irrigation area, North Queensland (Australia) show that seawater intrusion is far more sensitive to pumping rates and recharge than to aquifer properties (e.g., hydraulic conductivity), and compared to the effects of groundwater pumping, the effect of tidal fluctuations on saltwater intrusion can be neglected (Narayan et al., 2007). However, rare studies have focused on delineating the interactions among surface-ground-sea-waters in estuarine environment and the effects of vertical infiltration of seawater into the off-shore aquifer through river channel vs. the lateral landward migration of the freshwater-saltwater interface.

The data of China's marine environment bulletin released on March 2015 by State Oceanic Administration People's Republic of China showed that the major bays, including Bohai Bay, Liaodong Bay, Hangzhou Bay, are polluted seriously with the inorganic nitrogen and active phosphate as the major pollutants (SOA, 2015). Seawater intrusion in China is the most serious around the Circum-Bohai-Sea region. The escalating seawater intrusion in the future may be not a simple problem related to groundwater salinization in this region. It is likely to be more difficult to remediate groundwater pollution caused by the contaminated seawater. This study will take the Yang-Dai River coastal plain in Qinhuangdao City, Hebei province of north China, as an example to investigate groundwater salinization processes and interactions among surface water, groundwater and seawater, and the seawater intrusion caused by groundwater exploitation in Zaoyuan well field. Qinhuangdao is an important port and tourist city of northern China. In the past 30 years, many previous studies had done to investigate distribution of seawater intrusion and its influence factors using hydrochemical analysis of groundwater (Xu, 1986; Yang, 1994, 2008; Chen and Ma, 2002; Sun and Yang, 2007; Zhang, 2012) and numerical simulations (Han, 1990; Bao, 2005; Zuo, 2009). This study is a continuation of previous investigations of the coastal plain aquifers in Qinhuangdao.

Hydrol. Earth Syst. Sci. Discuss., https://doi.org/10.5194/hess-2017-617
Manuscript under review for journal Hydrol. Earth Syst. Sci.
Discussion started: 7 November 2017

Hydrochemical and stable isotopic compositions of collected water samples were analyzed for making up the knowledge gap of surface-, ground-and sea-water interactions in this region. This study aims to describe the conceptual model of the complex processes for the groundwater salinization of the coastal aquifers, to reveal the major aspects responsible for the increasing groundwater salinity in the coastal aquifers, and to obtain a conceptual model for deciphering the groundwater flow system of the study area. The results will be helpful for the further numerical simulations of coastal groundwater system. It is very significant for water resources management in the coastal plain.

2. Study area

The Yang-Dai River coastal plain (Fig. 1) covers approximately 200km^2 in the west side of Beidaihe District of Qinhuangdao City, the northeastern Hebei Province. It connects the eastern section of Yanshan Mountain and surrounded by mountains. The southern boundary of the study area is Bohai Sea. The plain become low from northwest to southeast and fan-shaped distribution of the piedmont- coastal inclined alluvial plain. Elevation ranges from 390 in the west and to 40-100 m in the north, and 25-40 in the east, and 25-1m in the south coastal region, with the average slope of 0.008. Zaoyuan well field, located in the southern edge of alluvial fan, was built in 1959 (Xu, 1986) as major water supply for this region. It is 4.3 km from the southeastern well field to Yang River estuary.

2.1 Climate and hydrology

The study area is in a warm and semi-humid monsoon climate. On the basis of a 56-a record in Qinhuangdao area, the mean annual rainfall is estimated to be 640 mm, the average annual temperature is about 11°C, and mean potential evaporation of 1469 mm. 75% of the total annual rainfall falls in July-September (Zuo, 2006). The average annual tide level is 0.86m (meters above Yellow Sea base level), the highest tide is 2.48m, and the lowest is -1.43m.

The Yanghe River and Daihe River originated from the Yanshan Mountains are the major surface water body in this area (Fig. 1). The river soared when heavy rains happened with short peak duration, whereas it became minimal flow or drying during the dry season. The Yang River is about 100 km long with the catchment area of 1029 km^2, and the average annual runoff of 1.11×10^8 m^3/a (Han, 1988). Dai River has the length 35 km and catchment area of 290 km^2, with annual runoff of 0.27×10^8 m^3/a and average gradient of 11.4‰. The two rivers flow into the southern Bohai Sea.

2.2 Geological and hydrogeological setting

Groundwater in this area mainly include fissure water in the bedrock and water in the Quaternary porous media. The bedrock fissure water is distributed in the north platform area. Its water abundance is mainly depended on the degree of weathering and the nature and regularity of fault zone. The strata outcropping in the west, north and eastern edge of the plain includes the Archean gneiss, Proterozoic mixed granite and Jurassic sandstone, shale and so on. The ex-Quaternary, which is exposed in the offshore area of the region, is mainly the Archean metamorphic granite, which is widely distributed. The mineral composition includes mainly quartz, feldspar, and biotite. The Quaternary sediments of the plain are mostly underlain by the Archean gneisses and Proterozoic mixed granites. The basement faults under the Quaternary cover mainly include the NE-trending fault and the NW-trending fault. The Quaternary aquifer system of the Yang-Dai River coastal plain is a complete groundwater system from the piedmont to the coast (see P-P' cross-section of Figure 2). Geological technics control the development and deformation of the sediments, the distribution of hot springs and geothermal anomalies. Fault zones are also the main channel for deep-water cycle and thermal convection.

The Quaternary sediments are widely distributed in the area. The bottom of the Holocene in most areas has clay or clay layers, which make the groundwater in the coastal zone under confined or semi-confined status. There are no regional, continuous aquitards between several aquifers. The thickness of the Quaternary strata has a range of 5-80 m, mostly 20-40 m, and up to more than 100 m near the coastline. The aquifer is mainly composed of medium sand, coarse sand and gravel with thickness of 10-20 m and water table depth of 1-4 m in the phreatic aquifer, and thickness of 10-30 m and water table depth of 1-5 m in the confined aquifer (Zuo, 2006). In the yearly peak season of agricultural water, the groundwater level decline sharply and reaches the lowest water table in April-May period, and become highest in January-February. The main sources of aquifer recharge are from rainfall infiltration, river water and irrigation return-flow, lateral subsurface runoff from the piedmont area. Apart from the phreatic water evaporation, groundwater pumping it the main pathway of groundwater discharge for agricultural, industrial, tourism and sanatorium's utilization. The general flow direction of groundwater is from northwest to south. Naturally, groundwater discharges into the river and the Bohai Sea.

The geothermal water near the fault zone discharges into shallow Quaternary sediments, which is the overlying strata in geothermal anomalous area (Hui, 2009). The temperature of thermal water range is 27-57 ºC in this low-to-medium temperature geothermal field (Zeng, 1991). The thickness of the overlying strata is varied from 24.6 to 58.8 m and consists of alluvial sand, gravel, clayey loam, clay and silt. The thermal water stored in the Archaeozoic granite and metamorphic rocks, which are composed of migmatite, gneiss, and amphibole plagio-gneiss (Pan, 1990). Major deep fracture zones are the good passage for the geothermal water movement (Yang, 2011). The heated groundwater in the deep zones could upward transport along the fault and mix with the cold groundwater in the Quaternary aquifers (Shen et al., 1993).

2.3 Environmental issues and seawater intrusion history

The shallow groundwater pumped from the Quaternary aquifer occupies 94% of the total groundwater exploitation, which is used for agricultural irrigation (accounts for 52% of the total groundwater use), industrial (32%) and domestic water (16%) (Meng, 2004). Many large and medium-sized reservoirs were built in the 1960s and 1970s and resulted in that the surface water was intercepted and the downstream runoff dropped sharply, even became dry in drought years. With the intensification of human socio-economic activities and growing urbanization, coupled with extended drought years (severe drought during 1976-1989 in north China) (Wilhite,1993; Han et al., 2015), increased groundwater exploitation to meet the ever-growing fresh water demands has resulted in groundwater level declining and seawater intrusion (SWI) in the coastal aquifers.

The pumping rate in the Zaoyuan well field was gradually increased from 1.25 million m^3/a in the early 1960s to 3.5 million m^3/a in the late 1970s, and beyond 10 million m^3/a in the 1980s. During 1966-1989, the major agricultural planting in this region is paddy field with big water consumption. The groundwater pumping time is mainly from May to October with pumping rate of 7~80,000 m^3/d, which was over-exploited and resulted in formation of groundwater level declining depression. In May 1986, the groundwater level in the depression center, which is located in Zaoyuan-Jiangying, was decreased to below -2 m.a.s.l. (meters above sea level), with the depression area, which has groundwater level below the sea level, covered 28.2 km^2. Since 1990, the rapid development of township enterprises in the 1980s (mainly refer to paper mills), groundwater over-exploitation in the west area (i.e. the groundwater pumping rate for paper mill development reached 55,000 m^3/d in 2002) resulted in the groundwater level depressions around Liushouying and Fangezhuang. The lowest groundwater level in the depression center in 1991 was up to -11.6 m.a.s.l., and -17.4 m.a.s.l. in 2002. After the implementation of "Transfering Qing River water to Qinhuangdao" project since 1992, the intensity of groundwater pumping became slowed down. The depression center moved to Liushouying area. The groundwater level of the depression center was recovered to -4.3 m.a.s.l. in July 2006. The shape of the depression was elliptical with the major axis of the EW direction. The depression area developed to 132.3km^2 in May 2004.

The groundwater quality of this area has become gradually salinized since the early 1980s. Chloride concentrations increased year by year. As early as 1979, seawater intrusion occurred in the Zaoyuan well field. The intrusion area with groundwater chlorine concentration greater than 250 mg/L has been developed to 21.8 km^2 in 1984, and 32.4 km^2 in 1991, 52.6 km^2 in 2004, 57.3 km^2 in 2007 (Zuo, 2006; Zang et al., 2010). The chloride concentration of groundwater pumped from this well field changed from 90 mg/L in 1963, 218 mg/L in 1978, 567 mg/L in 1986, 459 mg/L in 1995, and 1367 mg/L in 2002 (Zuo, 2006), 812 mg/L in July 2007 (this study). The distance of seawater intrusion into the inland reached 6.5 km inland in 1991, and developed to 8.75 km in 2008 (Zang et al., 2010). At the early 1990s, 16 of 21 pumping wells in the well field have been abundant due to the salinized water quality (Liang et al., 2010). 370 of 520 pumping wells has been abundant in the Yang-Dai River coastal plain during 1982-1991 (Zuo, 2006).

3. Methods

Totally 80 water samples were collected from the Yang-Dai River coastal plain, including 58 groundwater samples, 19 river water samples (from 12 sites), and 3 seawater samples during three sampling campaigns, namely, June 2008, September 2009 and August 2010. Groundwater samples pumped from 28 productive wells with well depth of 6-110m, including 7 deep wells, which has well depth more than 60m. The water sampling sites can be shown in Figure.1. In this study, we investigated cold groundwater from the productive wells. However, the geothermal water existing around Danihe cannot be ignored. The related data can be available and referenced from Zeng (1991) due to that we cannot obtain the hot water samples from the current geothermal field.

Measurements of some physical-chemical parameters (i.e. pH, temperature, and electrical conductivity (EC)) were conducted in situ using portable meter (WTW Multi 3500i). All water samples were filtered to 0.45 μm membrane filters before collection for analysis of hydrochemical composition. Two aliquots in polyethylene 100mL bottles at each site were collected: for major cation and anion analysis, respectively. Samples for cation analysis (Na, K, Mg and Ca) were added 6 N HNO_3 to prevent precipitation. Water samples were sealed and stored at 4 ºC until determination. Biocarbonates were determined by titration within 12 hours after sampling. The concentrations of cations and some trace elements (i.e. B and Sr) were analyzed by inductively coupled plasma-optical emission spectrometry (ICP-OES) on filtered samples in the chemical laboratory of the Institute of Geographic Sciences and Natural Resources Research (IGSNRR), Chinese Academy Sciences (CAS). Concentrations of major anions (i.e. Cl, SO_4, NO_3 and F) were analyzed by a High Performance Ion Chromatograph (SHIMADZU, LC-10ADvp) at the IGSNRR, CAS. The ion balance errors of the chemical results are less than 8%. The hydrochemical and physical data are shown in Table 1. The stable isotopes ($\delta^{18}O$ and δ^2H) of water samples were measured by a Finnigan MAT 253 mass spectrometer after on-line pyrolysis with a Thermo Finnigan TC/EA in the Stable Isotopes Laboratory of the IGSNRR, CAS. The results of $\delta^{18}O$ and δ^2H values shown in Table 1 were expressed in ‰ relative to international standards (V-SMOW (Vienna Standard Mean Ocean Water)). The analytical precision for δ^2H is ±2‰ and for $\delta^{18}O$ is ±0.5‰.

Saturation indices for common minerals (i.e. calcite, dolomite, and gypsum) were calculated using PHREEQC version 2.8 (Parkhurst and Appelo, 1999) to understand the saturation status of these minerals in the aquifer. Ionic delta values were calculated to further investigate the hydrogeochemical behavior that take place in the aquifer and modify groundwater hydrochemistry. The ionic delta values express enrichment or depletion of each ion's concentration relative to its theoretical concentration calculated from the Cl^- concentration of the sample for a conservative freshwater-seawater mixing system (Fidelibus et al., 1993; Appelo, 1994). The delta values have been used as effective indicators of coastal groundwater undergoing freshening or salinizing processes, accompanied by related water-rock interaction (prevailingly cation exchange). Cl^- can be regarded as a conservative tracer for the calculations mentioned below. The seawater contribution for each sample can be expressed by a fraction of seawater (f_{sw}), which can be calculated using (Appelo and Postma, 2005):

$$f_{sw} = \frac{C_{Cl,sam} - C_{Cl,f}}{C_{Cl,sw} - C_{Cl,f}} \qquad (1)$$

where $C_{Cl,sam}$, $C_{Cl,f}$, and $C_{Cl,sw}$ refer to the Cl^- concentration in the sample, freshwater, and seawater, respectively. Based on the f_{sw} value, the theoretical concentration ($C_{i,mix}$) of each ion in a water sample can be calculated by:

$$C_{i,mix} = f_{sw} \cdot C_{i,sw} + (1 - f_{sw}) \cdot C_{i,f} \qquad (2)$$

$C_{i,sw}$, and $C_{i,f}$ refer to the measured concentration of the ion i in the seawater and freshwater, respectively. The ionic delta value (ΔC_i) of ion i can be obtained by:

Hydrol. Earth Syst. Sci. Discuss., https://doi.org/10.5194/hess-2017-617
Manuscript under review for journal Hydrol. Earth Syst. Sci.
Discussion started: 7 November 2017

$$\Delta C_i = C_{i,sam} - C_{i,mix} \tag{3}$$

$C_{i,sam}$ - the measured concentration of the ion i in the water sample.

4. Results

4.1 Groundwater dynamics

Due to the different groundwater pumping rate and patterns, the variation trend of groundwater level has been different in the east and west areas of the Yang-Dai River coastal plain. In the east part, owing to the intensive exploitation in the Zaoyuan well field, the groundwater level was gradually declined to be lower than the sea level during the 1980s. The center of groundwater level depression was located in Zaoyuan-Jiangying region, with the groundwater level lower than -3 m.a.s.l. The local government commenced to reduce the exploitation after 1992. The groundwater level decreased slowly after 1995, even started to recovery in some wells as a result of pumping reduction. During the extreme drought year (1999), the consequential increased water demand made the groundwater level declined again in the east region. In the late 1980s, the groundwater level at the west region was still more than 0 m.a.s.l. But in the late 1990s, due to the fast development of the local paper mills as the big water consumers, the groundwater level dropped year by year and had big falling amplitude after 2000, resulting in the overall transfer of groundwater depression center to the western region (Liushouying-Fangezhuang). The groundwater level in this center was up to -14 m.a.s.l. in May 2002.

Based on the data from the three monitoring wells, the seasonal variation of groundwater level in this area can be seen from Figure 3. After 2000, the groundwater level in the east of the Yang-Dai River coastal plain was mainly affected by the groundwater pumping for agricultural and domestic water use. During March and June of each year, the shallow groundwater pumping as the major water source for irrigation has resulted in the fast dropped water level occurred between April and June, down to the lowest level of water throughout the year. As the rainy season started in July, groundwater pumping began to decrease. Groundwater level rise rapidly with the infiltration of irrigation return-flow and rainfall, lateral subsurface runoff from the surrounding aquifers. After the end of the rainy season (July to September), the water level continues to rise gently and reach the annual maximum water level during January and February. With the amount of recharge is reduced along with the increase of domestic water pumping, water level circularly slow down to the next agricultural peak. In addition to groundwater over-exploitation, climate change-induced recharge reduction in recent three decades has been also part of the cause of groundwater level declining, resulting in the seawater intrusion. The annual average rainfall varied from 639.7 mm (1954 - 1979) to 594.2 mm (1980-2010). It obviously finds that there is a significant decrease in rainfall over the last 30 years (Zhang, 2012). In general, the groundwater runoff intensity gradually decreases from the piedmont to the coastal region.

4.2 Water stable isotopes (δ^2H and $\delta^{18}O$)

19 water samples collected from Yang River and Dai River have $\delta^{18}O$ and δ^2H values ranging from -10.1 to -0.6‰ (mean= -5.4‰) and from -71~-11‰ (mean = -43‰), respectively. It seems that the stable isotopes composition have significant seasonal variation. For Yang River, 3 surface water sampled in relatively dry season (June 2008) were characterized by $\delta^{18}O$ and δ^2H values ranging from -5.5 to -1.1‰ (mean= -3.0‰) and from -49~-15‰ (mean = -31‰), respectively. Whereas 6 water samples sampled in wet season (August 2009 and September 2010) have $\delta^{18}O$ and δ^2H values ranging from -10.1 to -2.4‰ (mean= -6.6‰) and from -71~-21‰ (mean = -48‰), respectively. As to Dai River, in dry season, 3 surface water samples are characterized by $\delta^{18}O$ and δ^2H values ranging from -3.9 to -0.6‰ (mean= -2.6‰) and from -44~-11‰ (mean = -32‰), respectively; and in wet season, 7 surface water samples have $\delta^{18}O$ and δ^2H values ranging from -9.7 to -1.2‰ (mean= -6.6‰) and from -69~-12‰ (mean = -49‰), respectively. The water samples collected from Yang River and Dai River have similar stable isotopes composition.

56 groundwater samples are characterized by $\delta^{18}O$ and δ^2H values ranging from -11.0 to -4.2‰ (mean= -6.5‰) and from -76~-39‰ (mean = -50‰), respectively. Among them, 43 shallow groundwater samples have $\delta^{18}O$ and δ^2H values ranging from -11.0 to -4.2‰ (mean = -6.6‰) and from -76~-39‰ (mean = -50‰), respectively; 13 deep groundwaters have $\delta^{18}O$ and δ^2H values ranging from -7.8 to -5.1‰ (mean = -6.3‰) and from -58~-43‰ (mean = -50‰), respectively. For the shallow groundwater, during the dry season, 12 water samples have $\delta^{18}O$ and δ^2H values ranging from -7.2 to -4.2‰ (mean = -5.7‰) and from -56~-39‰ (mean = -48‰), respectively; during the wet season, 31 water samples are featured by $\delta^{18}O$ and δ^2H values with a range of -11.0 ~ -5.3‰ (mean = -6.9‰) and -76 ~ -43‰ (mean = -51‰), respectively. For the deep groundwater, during the dry season, 3 water samples have $\delta^{18}O$ and δ^2H values ranging from -5.3 to -5.1‰ (mean = -5.2‰) and from -47~-45‰ (mean = -46‰), respectively; during the wet season, 10 water samples are featured by $\delta^{18}O$ and δ^2H values with a range of -7.8 ~ -5.2‰ (mean = -6.6‰) and -58 ~ -43‰ (mean = -51‰), respectively.

The local meteoric water line (LMWL, $\delta^2H=6.6\ \delta^{18}O+0.3$, n=64, $r^2=0.88$) is based on δ^2H and $\delta^{18}O$

mean values of the monthly rainfall between 1985 and 2003 at Tianjin station some 120 km SW of Qinhuangdao City. The data were obtained from International Atomic Energy Agency/World Meteorological Organization (IAEA/WMO, 2006). Due to the similar climatic and coastal conditions between Tianjin and Qinhuangdao, this meteoric water line can be regarded as the local meteoric water line (LMWL) in this study. From Figure 4, it can be seen that surface water have more wide range of $\delta^{18}O$ and $\delta^{2}H$ values relative to groundwater. Water samples collected in wet season have more wide range of $\delta^{18}O$ and $\delta^{2}H$ values relative to water sampled in dry season. Most of water samples plot blow the LMWL. Seawater represents an end-member enriched in isotopes and plots far below the LMWL.

4.3 Water salinity and major dissolved ions

TDS (total dissolved solids) concentrations of the surface water samples from Dai River have a range of 0.3g/L~31.4g/L with 22-78% Na^{+}, 56-4% Ca^{2+} of total cations and 36-91% Cl^{-} of total anions, Ca•Na•Mg-Cl•HCO_3 to Na-Cl water type from the upstream to the downstream locations. The Cl^{-} concentrations varied from about 70 mg/L in the upstream to 16700 mg/L near the coastline. For Yang River, the collected water samples have TDS concentrations of 0.3-26.1 g/L with percentages (33-91%) of Cl^{-} concentrations (63.2-14953.5 mg/L) from the up-reach to the down-reach locations, with water types changed from Ca•Na-HCO_3•Cl•SO_4, Ca•Mg-Cl•SO_4•HCO_3 to Na-Cl. The nitrate contents range from 2.8 to 65.2 mg/L in the surface water samples.

Groundwater hydrochemistry can be modified the comprehensive effects from geological, climatic, hydrogeological processes and anthropogenic activities. In the early 1960s, groundwater pumped from the Zaoyuan well field was featured by the Ca-HCO_3 water type and chloride concentrations of 90-130 mg/L. In the early 1970s, individual wells appear slightly salinized. It has been deteriorated rapidly since the early 1980s. The chloride concentration of groundwater from water supply wells was 90mg/L in 1963, 218 mg/L in 1975, 385 mg/L in 1984, 456.3 mg/L in 1986, 459.5 mg/L in 1995, 928.3 mg/L in 2000, 1367 mg/L in 2002, and 1290.4 mg/L in 2005 (Zang et al., 2010). In this study, the shallow groundwater is characterized by TDS concentrations of 0.4-4.8 g/L with the percentage of Cl^{-} (34-77%), Na^{+} (12-85%), Ca^{2+} (5-69%) and water types varied from Ca-HCO_3•Cl, Ca•Na-Cl, Na•Ca-Cl to Na-Cl, which can been seen from Piper plot (Figure 5). The deep groundwater is featured by TDS concentrations of 0.3-2.8g/L, which is dominated by Ca (up to 77%) in the upstream area and Na (up to 85%) near coast, with water type distributed in series of Ca-Cl•HCO_3, Ca•Na-Cl and Na•Mg-Cl (Figure 5). The TDS of groundwater from the well field reaches

3.31 g/L with Na-Cl water type in the well G15. The relative high fracture of seawater occurs in the shallow well G10 and deep well G2, with *fsw* values of 12.95% and 5.35%, respectively. The nitrate contents have a range of 2.0-178.5 mg/L (mean 90.1 mg/L) for shallow groundwater, and 2.0-952.1 mg/L (mean 232.1 mg/L) for the deep groundwater, respectively, most of which seriously exceeds the WHO drinking water standard (50 mg/L).

There is a geothermal field around Danihe-Luwangzhuang area (Fig. 1). Hydrochemical features of thermal water are very distinct from cold water. The previous investigation has identified the buried geothermal water with high TDS in the fracture/fissure of deep metamorphic rock (Zeng, 1991). Due to the pumping wells for pumping thermal water were protected and not permitted to be sampled, we have to collect some data associated this geothermal field from the previous research. The geothermal field is controlled by the fault distribution under confined state. The thermal water flows along the fault zone and enters the Quaternary aquifer, forming hot salt water distributed around the spill point and expanded towards downstream. It can result in the similar hydrochemical characteristics between Quaternary salt groundwater and deep original thermal waters from bedrocks. The geothermal water is characterized by Ca•Na-Cl water type, 6.2-10.6 g/L of TDS and 7.4-8.7 of pH values. Cl^- concentrations range from 5.4 to 6.5 g/L, Na^+ from 1.7 to 2.0 g/L, Ca^{2+} from 1.6 to 1.9 g/L, F^- from 3.0 to 3.6 mg/L, Sr from 6.73 to 89.8 mg/L, Li from 0.43 to 1.58 mg/L, and SiO_2 from 44.0 to 48.3 mg/L (Hui, 2009). The groundwater samples, collected from the wells G8, G19, and G9 with different depths, are featured by Ca•Na-Cl water type with relative high TDS ranges (0.8-1.4 g/L, 1.3-1.6 g/L, and1.5-2.8 g/L, respectively) and Sr contents (1.1-1.9 mg/L, 4.9-7.1 mg/L, and 7.3-11.6 mg/L, respectively).

5. Discussions

5.1 Groundwater flow system and hydrochemical features

Generally, Quaternary groundwater system in the Yang-Dai River coastal plain is recharged by precipitation, irrigation return flow, river infiltration and lateral subsurface runoff from mountain-front region. Due to the natural geological function and human pumping activities, there have been interactions between groundwater and geothermal waters around Danihe area or between groundwater and seawater in the coastal area. The groundwater geochemical features are controlled by the complex hydrogeological conditions and these hydrological processes. The different sources of water bodies are characterized by different of stable isotopic and hydrochemical compositions, determining the groundwater salinization processes in this area.

The stable isotopes of O and H can be used to describe the groundwater origin and to identify the mixing processes between different water bodies. The slope of the best-fit regression line for collected groundwater samples (dashed line in Fig. 4) given as $\delta^2H=4.4\times\delta^{18}O-21.7$, which is significantly lower than either the local or global meteoric water lines. The deviation of groundwater and surface water lines from the LMWL has evidenced evaporative processes occurred during water infiltration and surface runoff. The composition of stable isotopes in groundwater samples collected in the relatively dry season has been narrower and enricher than that collected in the wet season. It could be resulted from evaporation processes during the infiltration of local irrigation return-flows in the dry season.

The composition of stable isotopes for thermal groundwater could be originated from precipitation, however, its ^{14}C age dating between 3.4-12.8ka with tritium content of less than 2 TU (Zeng, 1991), indicating thermal waters might be formed under cooler climate condition than present climate. The composition of stable isotopes of thermal groundwater are more depleted than that of cold groundwater, even lower than the cold groundwater from mountain-front area, indicating the thermal groundwater could be mainly originated from NW mountain area, where has higher elevation. The elevation range of recharge area for Danihe geothermal field is from 1200 to 1500 m.a.s.l obtained by Zeng (1991).

Fresh groundwater has depleted $\delta^{18}O$ and δ^2H values relative to seawater. Theoretically, the mixing of fresh groundwater and seawater should show a straight line connecting the two end members. Obviously, some surface water samples (e.g. S1, S2, S3, S7, S12) are the mixture with seawater. In this study area, there are three end members (namely, fresh groundwater, thermal groundwater and seawater), which has been evidenced by the previous studies (Han, 1988; Zeng, 1991). Thus, the diagram of $\delta^{18}O$ vs. Cl^- (Fig. 6) can be used to identify the mixing pattern among three end members. Fig. 6 shows the mixing lines between shallow fresh groundwater (G4) and seawater, between deep fresh groundwater (G25) and seawater, between shallow fresh groundwater and thermal water, and between deep fresh groundwater and thermal water. The shallow groundwater samples (e.g. G15, G10, G11, G14) collected from or around the Zaoyuan well field are characterized by mixing with seawater. The deep groundwater samples (e.g. G13, G2, G16, G14') collected from the coastal zone are also resulted from mixing with seawater. The sampling site of deep groundwater sample G29 is located between thermal field and the coastline and obviously affected by both of mixing processes. The groundwaters (e.g. G9, G19), sampled from the area affected by geothermal field are mixture between fresh cold groundwater with thermal waters. The mixing fraction (f_{sw})

of seawater has a range of 1.2~13.0% for the shallow brackish groundwater, and 2.6~6.0% for the deep brackish groundwater. f_{sw} reaches the highest percentage of 13% in the well G10, which is located in the north part of the well field.

At the late 1950s, groundwater pumped from the Zaoyuan well field was characterized by Ca-HCO_3 type water with Cl concentrations ranging from 130 to 170 mg/L. The hydrochemical data investigated in 1986 (Han, 1986) showed that there were mainly five water types in this study area, including Ca-HCO_3 type with TDS less than 0.5g/L distributed in the mountain-front area, Ca•Na-Cl•SO_4, Ca•Na•Mg-SO_4•Cl, or Na•Ca-Cl•SO_4 type water with TDS 0.4-0.7g/L distributed around the Zaoyuan well field and Wanggezhuang, Ca•Na-Cl type water with TDS 0.4-1.8g/L distributed around the geothermal field (Luwangzhuang) and Duzhai, Na-HCO_3 or Na-HCO_3•Cl type water with TDS 0.5-0.9g/L distributed the SW area close to the coastal zone, and Cl-Na type water with TDS 0.4-2.4g/L distributed in the coastal zone. Due to the disturbance of human activities, the current groundwater hydrochemistry has become more complex than that before. Compared salty water distributed 2 km away from coastline in the late 1950s, the distance has increased to about 7 km away from coastline. The Cl-Ca•Na or Cl-Ca type water type mainly distributed in the area affected by geothermal field, such as G5, G8, G19, G29, and G24, indicating the salinizing process during the mixing between cold groundwater and the thermal waters. In the upstream area, the groundwater samples (e.g. G7, G23, G25) have feature of Ca•Mg•Na-Cl•SO_4, Ca-Cl•SO_4, and Ca-Cl•HCO_3 type, not the Ca-HCO_3 type in the 1980s. It suggests that the salinized composition has resulted from the anthropogenic pollution. The groundwater samples (e.g. G10, G11, G15, G26) collected from the well field show the feature of Cl-Na• (Ca) type water with TDS 1.2-4.8 g/L. The samples (e.g. G1, G2, G3, G4, G12, G22, G14, G14') collected from the coastal zone show the water type of Na-Cl or Na•Ca-Cl•SO_4 or Ca•Na•Mg-Cl•SO_4, indicating that, apart from seawater intrusion, the anthropogenic pollution also plays important role on modifying the groundwater chemistry.

The seawater from Bohai Sea has relatively higher NO_3^- concentrations (810 mg/L in this study, up to 1092 mg/L in the coastal seawater of Dalian, Han et al., 2015) due to wastewater discharge into the sea. NO_3^- concentration of groundwater in the well field increased from 5.4 mg/L in May 1985 to 146.8~339.4 mg/L in Aug 2010, while the concentration of seawater in this area changed from 57.4 mg/L in May1985 to 810.1 mg/L in Aug 2010. The diagram (Fig. 7) of Cl^- vs. NO_3^- concentration of groundwater can be used to identify the different mixing trend in this study area, including the mixing process with contaminated seawater, and the anthropogenic NO_3-sources (e.g. domestic/industrial wastewater discharge, NO_3^--bearing fertilizer input through precipitation infiltration and the irrigation return-flow) in the inland area. It can be seen from Fig. 7 that the major source of NO_3^- in groundwater is from anthropogenic input, with the exception of G10 and G15 mixing with seawater in the well field. The deep groundwater (e.g. G9, G14') is also contaminated by higher NO_3^- concentrations, which is likely associated with the abandoned wells. According to one investigation by Zang et al.(2010), 14 of 21 pumping wells in the Zaoyuan well field have been abandoned due to the salinized water quality, and 307 pumping irrigation wells (occupied 2/3 of total pumping wells for irrigation) have been abandoned. However, the local department has not made any measure to deal with those abandoned wells.

5.2 Groundwater salinization processes

5.2.1 Development of seawater intrusion and associated hydrochemical behavior

The intensively pumping groundwater from the Quaternary aquifer of Yang-Dai River coastal plain has resulted in the development of groundwater depression cones from Zaoyuan well field to Fangezhuang, with the aggravation of seawater intrusion in this region. In the 1950s, the seawater intrusion in the study area was only occurred within 2 km distance from the coastline, and it expanded to over 5 km distance in the 1980s. In 1986, the groundwater depression cone centered in the Zaoyuan well field was characterized by 6 meters depths below the sea level, with the water level -3 m.a.s.l. The enclosed area by 0 m.a.s.l water level contours covered 10 km^2. The original Ca-HCO_3 type water changed to Ca•Na-Cl type. Apart from the intensive exploitation fresh groundwater from coastal aquifer, the successive drought (1976-1989) also played important roles on controlling the groundwater recharge and exacerbating seawater intrusion in the coastal area of north China (Wilhite, 1993; Han et al., 2015). In this study area, the annual mean precipitation was 668.7 mm during 1954-1995, the Cl concentrations was ranging from 130 to 170 mg/L in the Zaoyuan well field. Whereas the annual mean precipitation reduced to 559.7 mm during 1996-2011, resulting in Cl concentration in the well field up to 550 mg/L in May 1986, and 812 mg/L in July 2006. It has seriously threatened the safety of water supply in this region. The seawater intrusion in the coastal aquifer shows the wedge-shaped body and has vertically characterized by freshwater in the upper part and salt water in the lower part of shallow aquifer. Since 2002, with the establishment of anti-tide dam in the Yang River estuary area, it has good effect on preventing the horizontal pouring seawater into riverway. Thus, the seawater intrusion is mainly caused by lateral inflow of seawater in the aquifer.

According to the guidelines of drinking water standards from China Environmental Protection

Authority (GB 5749-2006) or US EPA or WHO, the guideline of chloride concentration for drinking water is 250 mg/L. Most groundwater distributed in the seawater intrusion area cannot be used for irrigation, the source of drinking water and industrial utilization. It has enhanced the scarcity of fresh water resources in this region by vicious cycle of groundwater level decline → seawater intrusion → groundwater salinization → groundwater level decline again. This will also influence the surface water runoff. How to judge the criterion of seawater intrusion? Generally, 250 mg Cl/L can be regarded as the intruded standard, and more than 1000 mg Cl/L as the serious intrusion (Jiang and Li, 1997; Zhuang et al., 1999). Some studies took the TDS (>1000 mg/L) as the intruded standard (e.g., Xue et al., 1997; Zhang and Peng, 1998). Water type can also be used as the intruded standard, such as Ca-Cl type water occurs during seawater intrusion into freshwater aquifers, and Na-HCO_3 type water displays during flushing of the mixing zone by freshwater (Appleo and Postma, 1993). Additionally, the multi-hydrochemical ionic ratios can also provide important confirmation of hydrogeochemical processes modifying groundwater chemistry during seawater intrusion (Vengosh et al., 1997; Jones et al., 1999). However, the frequent anthropogenic activities modified coastal hydrologic dynamics and hydrogeochemical characteristics to great extent. For instance, with except of modern seawater, the sources of chloride in groundwater system could be derived from paleoseawater relics in aquifers, infiltration of agricultural return flow with fertilizer solutions, and discharge of industrial and domestic wastewater.

Hydrogeochemical facies evolution diagram (HFE-D) proposed by Giménez-Forcada (2010) can be used to analyze the phase of seawater intrusion or freshening and its dynamics. From Fig. 8, it can be seen that most brackish groundwaters (e.g., G11, G16, G17, G20, G25, G28, G29) have evolved in the series of Ca-HCO_3 → Ca-Cl→ Na-Cl facies under the intrusion period. Locally, several water samples (e.g., G1, G12, G26) collected from the interfluve area have been characterized by freshening process. Deep groundwater G11 sampled from the well field shows being under salinizing period in the relatively dry season, and under freshening period in the relatively wet season. In the coastal zone, the river water has obvious mixing trend between end members. Some shallow groundwaters (e.g., G2, G4, G10, G13, G15) are close to the mixing line between end members on this figure, indicating significant mixing with seawater. The groundwaters (G10, G11, G15, G26) collected from the productive wells of the Zaoyuan well field display the different processes occurring in salinizing or freshening stages, indicating that the heterogeneous hydrogeological conditions could be responsible for this distinguished patterns.

The calculated results of saturated indices (Fig. 9) show that that SI_{cal} and SI_{dol} have some deviation from equilibrium (-0.4 to +0.5 for SI_{cal}, and -0.5 to +0.5 for SI_{dol}). The distribution of SI_{cal} and SI_{dol} is related to the sampling period. In the wet season, most of water samples are characterized by SI_{cal} <0 and SI_{dol} <0, suggesting they are under unsaturated for these minerals, while in the dry season, most of water samples are under saturated with respect to these minerals. In contrast, all sampled groundwater had negative saturation indices with respect to gypsum (SI_{gyp}<0), indicating that these water samples are under-saturated with respect to gypsum. The plots (Fig. 10 a-f) of ionic molar ratios (Na/Cl, SO_4/Cl, Mg/Ca, Ca/(SO_4+HCO_3), Ca/SO_4, and (Ca+Mg)/Cl) can be used to further reveal the groundwater salinized processes and dominated hydrochemical behavior. The brackish groundwaters in this study area have an enriched Ca^{2+} (i.e., the ratio of Ca/(HCO_3+SO_4)>1 with low ratios of Na/Cl and SO_4/Cl as the seawater proportion in the mixture increases. As shown in Fig. 10a, Na/Cl ratios of brackish groundwater affected by seawater intrusion are usually lower than the ratio (0.86) of modern seawater. The high Na/Cl ratios (>1) could be typical of anthropogenic sources (i.e., domestic waste waters). When seawater intrudes into coastal freshwater aquifers, Ca^{2+} on the clay-bearing sediments can be replaced by Na^+:

$$2Na^+ + Ca\text{-}X_2 \rightarrow 2Na\text{-}X + Ca^{2+}$$

This process can decrease the Na/Cl ratios and increase the (Ca+Mg)/Cl ratios. The dolomitization process can be described by the transformation reaction (Appelo and Postma, 2005):

$$2CaCO_3 + Mg^{2+} = CaMg(CO_3)_2 + Ca^{2+}$$

It can result in Ca-enrichment over Mg in solution and that Mg/Ca ratios decreases. This process may also be characterized by Ca-Cl water type.

To explain the enrichment in Ca^{2+} relative to SO_4^{2-} concentrations, observed in most water samples (Fig. 10e), gypsum dissolution (SI_{gyp}<0) can be coupled by cation exchange reactions under the interaction with clay stratum and calcite precipitation with incongruent dissolution of dolomite and gypsum. Additionally, due to the ORP values ranging from 3 to 74 mV for 18 of 22 water samples collected in August 2010, the sulfate reduction under anaerobic conditions may be responsible for relatively high Ca/SO_4 and low SO_4/Cl ratios. Generally, low Na/Cl, SO_4/Cl and high Ca/(HCO_3+SO_4) (>1) ratios are further indicator of the arrival of seawater intrusion.

ΔNa is negative in most samples of this area (Fig. 11a and Fig. 12a). The depletion of Na^+ could be caused by the inverse cation exchange taken place with the clay sediments. This exchange produces Ca release to the solution during the seawater intrusion. The positive ΔCa and ΔMg may be due to the dissolution of calcite, dolomite and gypsum present in the aquifer strata. Water flushing during aquifer recharge can result in positive △Na and negative △Ca and/or △Mg (Fig. 11a). For some water samples, the Ca enrichment is not accompanied by Na depletion, which could be caused by dolomitization (Ca enrichment with Mg depletion) (Fig. 12b). The excess of SO_4 compared to conservative mixing (Fig. 11d) can be explained by redissolution of the precipitated gypsum along the mixing front.

5.2.2 Mixing between thermal and cold groundwater

Sea level rose by about 100 m since the end of the last glacial period (18,000 years, 18 ka BP) and stabilized around 5 ka BP in the eastern China (Yang, 1996). The marine sediments could not be found in the geothermal field, indicating the transgression in the geologic history did not occur around Danihe area (Zeng, 1991). However, the fracture and structural fissure developed well in this study area became the major subsurface pathway of seawater intrusion. The previous studies have revealed that the geothermal waters in this area are characterized by the features of residual seawater and modern precipitation (Zeng, 1991; Hui, 2009). The results of ^{14}C age dating for the geothermal waters in this area are ranging from 3.4 ka to 12.8 ka with lower tritium contents (less than 2TU) (Zeng, 1991). The Piper plot (Fig. 5) shows CaNa-Cl type water for the geothermal waters. It is noteworthy that the geothermal water from Danihe geothermal field has higher Sr concentrations (up to 89.8 mg/L) relative to that in seawater (5.4-6.5 mg/L in this study), due to the Sr-bearing minerals (i.e., celestite, strontianite) with Sr contents of 300-2000 mg/kg present in the bedrock (Hebei Geology Survey, 1987). The mixture waters sampled from the geothermal field in this study also have the higher Sr concentrations relative to seawater, i.e., G9 with Sr concentrations ranging from 7.4 to 11.6 mg/L, and G19 from 4.9 to 7.1 mg/L. The diagram of chloride versus strontium concentrations of different water samples (Fig. 13) shows that the groundwater samples (e.g., G9, G19) collected from the geothermal field have obviously been characterized by closing to mixing line between fresh cold- and thermal-groundwater. Some waters (G16, G20, G29) sampled from the downstream area also close to this mixing line, indicating the thermal water overflows into the coastal aquifers in different depths. The water samples collected from the well field are located between two mixing lines (Fig. 13), suggesting the groundwater in the well field simultaneously suffered from the mixing with thermal water and obvious seawater intrusion. Additionally, the points of water samples (G5, G8, G9, and G19), collected from the geothermal field, mainly occurs on the HFE-D (Fig. 8) in the *12* (MixCa-Cl) and *16* (Ca-Cl) facies zones, indicating these waters have been modified by the reverse base-exchange reactions.

As both Cl and Br are not affected by water-rock interactions and usually behave conservatively, the

Cl/Br ratio can be used as a reliable tracer to study the processes of evaporation and salinization of water (Edmunds, 1996; Jones et al., 1999). Standard seawater (Cl/Br molar ratio=650.8) may be distinguished from relics of evaporated seawater (normally less than 669.3), input of evaporite dissolution (more than 2256) and anthropogenic pollution (e.g., sewage effluents, Cl/Br ratios up to 1805; Vengosh and Pankratov, 1998) or agricultural return-flows with low Cl/Br ratios (Jones et al., 1999). It can be seen from Fig. 14 that the points of the thermal waters lie lower than the ratio line of standard seawater, indicating that they are affected by mixing with relics of evaporated seawater. The points of cold groundwaters (G9, G19) sampled from the geothermal field display between the seawater and the thermal waters, indicating these cold waters are mixture between cold groundwater and the thermal water, which has relics of evaporated seawater. However, it cannot exclude adding the Br inputs into groundwater system through the pesticides application of the pronounced agricultural activity (Davis et al., 1998), this effect could lower the Cl/Br ratios of the groundwaters. The groundwater sample G10 in the well field shows the feature of high Cl/Br ratio in Fig. 14, indicating obvious anthropogenic inputs (e.g., discharge domestic wastewater) occurring in the shallow aquifers around the well field.

5.2.3 Interaction between surface- and ground-water

Coastal zones encompass the complex interaction among different waters (i.e., river water, seawater, groundwater, rainfall water). The interaction between surface- and ground-water in the Yang-Dai River coastal plain is usually ignored by the previous studies. However, understanding how surface water interacts with the groundwater is essential for managing freshwater resources. Groundwater depression cone below the sea level has formed in the early 1980s. Due to the irrigation supported by transfer of surface water from the upper and middle stream of Yang-Dai River, the amount of surface water discharged into the Bohai Sea declined to great extent. Under the tide effects, seawater can be poured into the estuary of the downstream section of the rivers, resulting in the river bed filled with saltwater, which can cause mixing between river water and seawater. The results of water chemistry analysis from two river sections show that the distribution of salt water reached more than 10 km above the estuary of the Yang River, and about 4 km above the estuary of the Dai River (Han, 1988). It leaded to that the seawater simultaneously intruded into the coastal aquifers through not only the lateral subsurface flow from coastline to the inland but also vertical infiltration from the riverbed to both sides of the river. The hazard caused by the latter pattern had been more serious than the former pattern, before the establishment of anti-tide dam at the estuary of Yang River. Currently, the seawater-intruded distance towards inland has been controlled within 4 km away from the coastline.

The stable isotope compositions of different water samples (Fig. 4) display that the points of most surface water samples are deviated from the LMWL to the right, indicating that these waters are likely to be subject to evaporation to different degrees. The points of surface water samples (S1, S2, S3, and S7) in Fig.4 close to the compositions of local seawater, indicating the pronounced mixing process with seawater for these surface waters. However, the samples S2, S6, S8, and S9 have the depleted compositions of stable isotopes, probably resulting from the exchange between them and local groundwater. S12, located at the estuary area, has variable compositions due to the sampling seasons. HFE-D shows that most of surface water samples are close to the mixing line between end members (freshwater and seawater). S9 is significantly characterized by salinization process probably due to the interaction with ambient groundwater. It can be seen from the relationship between ionic delta values and seawater proportions for the water samples (Fig. 11) that G1, G11, G12, G14', G26, G29, due to these wells close to the river or located at the flat interfluve, may be dominated by the obvious freshening process. While G2, G3, and G16 under the salinizing process could be subject to the vertical infiltration of saltwater in the river. The points of surface waters (S1, S2, S3, and S7) on Fig. 4 and Fig. 8 are distributed along the mixing line between fresh- and sea-water end members. It is due to the direct mixture occurs in the riverway. S12 sampled from the Dai River estuary may be contaminated by the wastewater discharge with higher Sr concentration relative to seawater. By contrast, surface water from the Dai River have higher seawater proportions compared with that from Yang River, owing to that the local government did not establish anti-tide dam in the Dai River estuary. G1, G2, G3, G10 and G13 collected from coastal zone are obviously mixed with seawater with closing to the mixing line between seawater and freshwater in Fig. 13.

5.3 Conceptual model of groundwater flow patterns

Generally, groundwater in this study area is mainly originated from precipitation, river infiltration, lateral subsurface runoff, upflow of geothermal waters and seawater intrusion in the coastal area. The associated hydrological processes driven by the natural (hydrologic, geologic, climatic) changes and anthropogenic activities have resulted in groundwater salinization processes, along with the complex hydrogeochemical characteristics of groundwater system. Groundwater changes from Ca-HCO_3 type water in the piedmont area to the Na-Cl type water in the coastal area.

Hydrology and Earth System Sciences
Open Access
Discussions

A conceptual model groundwater flow system in the Yang-Dai River coastal plain can be summarized in Fig. 15. Four subsurface processes, including seawater intrusion, return-flow of agricultural irrigation, mixing with geothermal water and interaction between surface water and groundwater/seawater, could be responsible for the groundwater salinization in this area. Two aspects of seawater intrusion, identified by depleted ΔNa and enriched ΔCa with Ca-Cl type water and $Ca/(HCO_3+SO_4)>1$ and lower Na/Cl and SO_4/Cl relative to these ratios of seawater, can be delineated, namely vertical infiltration of saltwater inflow towards the inland estuary and lateral inflow of seawater driven by over-pumping groundwater from fresh aquifers. Irrigation return-flow from local groundwater can cause groundwater nitrate pollution (up to 340 mg/L NO_3^- in groundwater of this area) due to the infiltration and dissolution of fertilizers. Geothermal water with high TDS, F, and Sr concentrations flows into the Quaternary aquifers, mixing with cold groundwater, and transports to the downstream area of Yang River Basin. Additionally, the interaction between surface- and ground-water can cause seasonal flushing local groundwater in the upstream interfluve or lead to saltwater infiltration affected by tide/surge along the riverbed at the estuary.

6. Conclusions

It has been recognized that groundwater in the Quaternary aquifers of the Yang-Dai River coastal plain is the important water resource for agricultural irrigation, urban and tourism development and industrial utilization. Natural climate change (e.g., continuous drought, overflow of geothermal water) and human activities have made the problem of groundwater salinization in this area increasingly prominent, even resulting in the closure of the Zaoyuan well field. Based on the analysis of hydrochemical and stable isotopic compositions of different water bodies, including surface water, cold groundwater, geothermal water, and seawater, we delineated the groundwater flow system and groundwater salinization processes. Seawater intrusion is the main aspect responsible for the groundwater salinization in the coastal zone, including the vertical saltwater infiltration along the riverbed into aquifers, which is affected by the tide/surge process, and the lateral seawater intrusion caused by pumping for fresh groundwater. The overflow of the high mineralized thermal water into the Quaternary aquifers along the fault zone mixes with the cold groundwater and makes it salinized. The thermal water has characterized by lower Cl/Br ratios and higher Sr concentrations relative to seawater. It cannot be ignored that the salinization or nitrate pollution from the anthropogenic activities (e.g., agricultural irrigation return-flow with solution of fertilizers). Additionally, the interaction between surface- and ground-water can also affect the groundwater salinization in this area. Different approaches of hydrochemical analysis, such as Piper plot, HFE-D, major ionic ratios (Na/Cl, SO_4/Cl, Ca/SO_4, (Ca+Mg)/Cl, Ca/(SO_4+HCO_3), Cl/Br) and Sr, were used in this study to identify the different hydrogeochemical reactions and freshening or salinizing processes in the Quaternary aquifers.

Groundwater salinization has become a prominent water environment problem in the coastal area of north China, which has caused the further paucity of fresh water resources and has become the bottleneck of urban development to a certain extent. Since the 1990s, the local government has begun to pay attention to the development of seawater intrusion, and the irrational exploitation has been restricted. The Zaoyuan well field has ceased to pump groundwater since 2007. The anti-tide dam has been established in the Yang River estuary area in 2002, effectively intercepting the seawater pouring into riverway during the tide/surge period. These actions have made the rate of intrusion slowed down. The joint use of surface water and groundwater with reasonable exploitation program is essential and economical for the local water resources management. However, the quantitative understanding to the vertical and lateral saltwater intrusion into fresh aquifers should be obtained from further continuous groundwater monitoring and numerical groundwater flow and transport modeling. This study would be benefit the local agricultural development and groundwater resources management.

Acknowledgement

This research was supported by Zhu Kezhen Outstanding Young Scholars Program in the Institute of Geographic Sciences and Natural Resources Research, Chinese Academy of Sciences (CAS) (grant number 2015RC102), and Outstanding member program of the Youth Innovation Promotion Association, CAS (grant number 2012040). The authors appreciate the helpful field work and data collection made by Mr Yang Jilong from Tianjin Institute of Geology and Mineral Resources, Dr. Wang Peng and Dr Liu Xin from Chinese Academy of Sciences.

References

An T.D., Tsujimura M., Phu V.L., Kawachi A., Ha D.T., 2014. Chemical Characteristics of Surface Water and Groundwater in Coastal Watershed, Mekong Delta, Vietnam. The 4th International Conference on Sustainable Future for Human Security, SustaiN 2013. Procedia Environmental Sciences. 20:712-721.

Appelo C. A. J., Postma D., 1993. Geochemistry, Groundwater and Pollution, first edition. A. A. Balkema, Brookfield, Vt.

Appelo C.A.J., 1994. Cation and proton exchange, pH variations, and carbonate reactions in a freshening aquifer. Water Resour. Res., 30, 2793-2805.

Appelo C.A.J., Postma D., 2005. Geochemistry, Groundwater and Pollution, second edition. Taylor & Francis Group.

Bao J., 2005. Two-dimensional numerical modeling of seawater intrusion in Qinhuangdao Region. Master's

Hydrol. Earth Syst. Sci. Discuss., https://doi.org/10.5194/hess-2017-617
Manuscript under review for journal Hydrol. Earth Syst. Sci.
Discussion started: 7 November 2017

Thesis. Tongji University, Shanghai, China. (Chinese with English abstract)

Barbecot F., Marlin C., Gibert E., Dever L., 2000. Hydrochemical and isotopic characterisation of the Bathonian and Bajocian coastal aquifer of the Caen area (northern France). Applied Geochemistry. 15:791-805.

Bobba A.G., 2002. Numerical modelling of salt-water intrusion due to human activities and sea-level change in the Godavari Delta, India. Hydrological Sciences. 47(S), S67-S80.

Bobba A.G., 2002. Numerical modelling of salt-water intrusion due to human activities and sea-level change in the Godavari Delta, India. Hydrological Sciences. 47(S), S67-S80.

Bouchaou L., Michelot J.L., Vengosh A., Hsissou Y., Qurtobi M., Gaye C.B., Bullen T.D., Zuppi G.M., 2008. Application of multiple isotopic and geochemical tracers for investigation of recharge, salinization, and residence time of water in the Souss–Massa aquifer, southwest of Morocco. Journal of Hydrology. 352: 267-287.

Brockway R., Bowers D., Hoguane A., Dove V., Vassele V., 2006. A note on salt intrusion in funnel-shaped estuaries: Application to the Incomati estuary, Mozambique. Estuarine, Coastal and Shelf Science. 66:1-5.

Cary L., Petelet-Giraud E., Bertrand G., Kloppmann W., Aquilina L., Martins V., Hirata R., Montenegro S., Pauwels H., Chatton E., Franzen M., Aurouet A., the Team. Origins and processes of groundwater salinization in the urban coastal aquifers of Recife (Pernambuco, Brazil): A multi-isotope approach. Science of the Total Environment. 530-531:411-429.

Chen M., Ma F., 2002. Groundwater resources and the environment in China. Seismological Press. Beijing. pp255-281. (in Chinese)

Craig, H., 1961. Standard for reporting concentration of deuterium and oxygen-18 in natural water. Science 133, 1833–1834.

Creel L., 2003. Ripple effects: Population and coastal regions. Population Reference Bureau. pp1-7.< http://www.prb.org/Publications/Reports/2003/RippleEffectsPopulationandCoastalRegions.aspx>

de Montety V., Radakovitch O., Vallet-Coulomb C., Blavoux B., Hermitte D., Valles V., 2008. Origin of groundwater salinity and hydrogeochemical processes in a confined coastal aquifer: Case of the Rhône delta (Southern France). Applied Geochemistry. 23: 2337-2349.

Edmunds W. M., 1996. Bromine geochemistry of British groundwaters. Mineral. Mag., 60, 275–284.

El Yaouti F., El Mandour A., Khattach D., Benavente J., Kaufmann O., 2009. Salinization processes in the unconfined aquifer of Bou-Areg (NE Morocco): A geostatistical, geochemical, and tomographic study. Applied Geochemistry. 24:16-31.

Ferguson G., Gleeson T., 2012. Vulnerability of coastal aquifers to groundwater use and climate change. Nature Climate Change. 2, 342-345.

Fidelibus M.D., Giménez E., Morell I., Tulipano L., 1993. Salinization processes in the Castellon Plain aquifer (Spain). In: Custodio, E., Galofré, A. (Eds.), Study and Modelling of Saltwater Intrusion into Aquifers. Centro Internacional de Métodos Numéricos en Ingeniería, Barcelona, pp267-283..

Garing C., Luquot L., Pezard P.A., Gouze P., 2013. Geochemical investigations of saltwater intrusion into the coastal carbonate aquifer of Mallorca, Spain. Applied Geochemistry. 39:1-10.

Ghassemi F., Chen T.H., Jakeman A.J., Jacobson G., 1993. Two and three-dimensional simulation of seawater intrusion: performances of the "SUTRA" and "HST3D" models. AGSO J. Aust.Geol.Geophys. 14(2-3):219-226.

Ghiglieri G., Carletti A., Pittalis D., 2012. Analysis of salinization processes in the coastal carbonate aquifer of Porto Torres (NW Sardinia, Italy). Journal of Hydrology. 432-433:43-51.

Giambastiani B.M.S., Antonellini M., Oude Essink G.H.P., Stuurman R.J., 2007. Saltwater intrusion in the unconfined coastal aquifer of Ravenna (Italy): A numerical model. Journal of Hydrology. 340:91-104.

Giménez-Forcada E., 2010. Dynamic of sea water interface using hydrochemical facies evolution diagram, Ground Water. 48, 212-216.

Gingerich S., Voss C., 2002. Three-dimensional variable-density flow simulation of a coastal aquifer in southern Oahu, Hawaii, USA, in Proceedings SWIM17 Delft 2002, edited by R. Boekelman, pp.93-103, Delft Univ. of Technol., Delft, Netherlands.

Han D., Post V.E.A., Song X., 2015. Groundwater salinization processes and reversibility of seawater intrusion in coastal carbonate aquifers. Journal of Hydrology. 531:1067-1080.

Han D.M., Kohfahl C., Song X.F., Xiao G.Q., Yang J.L., 2011. Geochemical and isotopic evidence for palaeo-seawater intrusion into the south coast aquifer of Laizhou Bay, China. Applied Geochemistry, 26(5):863-883.

Han Z., 1988. Seawater intrusion into coastal porous aquifer- a case study of the alluvial plain of Yang River and Dai River in Qinhuangdao City. China University of Geosciences, Beijing, China. (Chinese with English abstract)

Han Z., 1990. Controlling and harnessing of the seawater intrusion the alluvial plain of Yang River and Dai River in Qinhuangdao.Geoscience (Journal of Graduate School, China University of Geosciences). 4(2):140-151. (Chinese with English abstract)

Hebei Geology Survey, 1987. Report of regional geological and tetonic background in Hebei Province. Internal materials.

Hui G., 2009. Characteristics and formation mechanism of hydrochemistry of geothermal water in Danihe, Funing District of Qinhuangdao region. Science & Technology Informaion. 9:762-763. (in Chinese)

IAEA/WMO, 2006. Global Network of Isotopes in Precipitation. The GNIP Database, Vienna. <http://www-naweb.iaea.org/napc/ih/IHS_resources_gnip.html>.

IPCC, Climate Change 2007: The Physical Science Basis, Contribution of Working Group I to the Fourth Assessment Report of the Intergovernmental Panel on Climate Change, S. Solomon et al., Eds. (Cambridge Univ. Press, Cambridge, 2007).

Jiang A., Li D., 1997. Characteristics of shallow groundwater hydrochemistry modified by saltwater intrusion in the south coast plain of Laizhou Bay. Acta Oceanologica Sinica.19(4):142-147. (in Chinese)

Jones B.F., Vengosh A., Rosenthal E. Yechieli Y., 1999. Geochemical investigations. In: Bear et al. (eds) Seawater Intrusion in Coastal Aquifers - Concepts, Methods and Practices, pp51-72.

Langevin C.D., Zygnerski M.R., White J.T., Hughes J.D., 2010. Effect of sea-level rise on future coastal groundwater resources in southern Florida, USA. SWIM21-21st Salt Water Intrusion Meeting. Azores, Portugal., June 21-26, 2010. Pp125-128.

Masterson J.P., 2004. Simulated interaction between freshwater and saltwater and effects of ground-water pumping and sea-level change, Lower Cape Cod aquifer system, Massachusetts: U.S. Geological Survey Scientific Investigations Report 2004-5014, 72 p.

Mazi, K., Koussis, A.D., Destouni, G., 2014. Intensively exploited Mediterranean aquifers: proximity to tipping points and control criteria for sea intrusion. Hydrol. Earth Syst. Sci. 18, 1663-1677.

Meng F., 2004. Rational development of groundwater resources on the coastal zone of Qinhuangdao area. Marine Geology Letters. 20(12):22-25. (Chinese with English abstract)

Mondal N.C., Singh V.P., Singh V.S., Saxena V.K., 2010. Determining the interaction between groundwater and saline water through groundwater major ions chemistry. Journal of Hydrology. 388:100-111.

Hydrol. Earth Syst. Sci. Discuss., https://doi.org/10.5194/hess-2017-617
Manuscript under review for journal Hydrol. Earth Syst. Sci.
Discussion started: 7 November 2017

Hydrology and Earth System Sciences
Open Access
Discussions

Montenegro S.M.G., de A. Montenegro A.A., Cabral J.J.S.P., Cavalcanti G., 2006. Intensive exploitation and groundwater salinity in Recife coastal plain (Brazil): monitoring and management perspectives. Proceedings 1st SWIM-SWICA Joint Saltwater Intrusion Conference, Cagliari-Chia Laguna, Italy - September 24-29, 2006. pp79-85.

Moore W.S., 1996. Large groundwater inputs to coastal waters revealed by 226Ra enrichments. Nature 380,612-214.

Narayan K.A., Schleeberger C., Bristow K.L., 2007. Modelling seawater intrusion in the Burdekin Delta Irrigation Area, North Queensland, Australia. Agricultural Water Management. 89:217-228.

Pan G., Yang Y., Zhang L., 1990. Survey report of geothermal water in Qinhuangdao city of Hebei Province. Team of mineral hydrological and engineering geology from the Bureau of Geology and mineral Resources of Hebei Province, China. (in Chinese)

Parkhurst D.L., Appelo C.A.J., 1999. User's Guide to PHREEQC – A Computer Program for Speciation, Reaction-Path, 1D-Transport, and Inverse Geochemical Calculation. US Geol. Surv. Water-Resour. Invest. Rep. 99-4259.

Post V.E.A., 2005. Fresh and saline groundwater interaction in coastal aquifers: Is our technology ready for the problems ahead? Hydrogeology Journal. 13:120-123.

Price R.M., Herman J.S., 1991. Geochemical investigation of salt-water intrusion into a coastal carbonate aquifer: Mallorca, Spain. Geological Society of America Bulletin. 103:1270-1279.

Pulido-Leboeuf P., 2004. Seawater intrusion and associated processes in a small coastal complex aquifer (Castell de Ferro, Spain). Applied Geochemistry. 19:1517-1527.

Radhakrishna I., 2001. Saline fresh water interface structure in Mahanadi delta region, Orissa, India. Environmental Geology. 40(3):369-380.

Rahmawati N., Vuillaume J., Purnama I.L.S., 2013. Salt intrusion in Coastal and Lowland areas of Semarang City. Journal of Hydrology. 494:146-159.

Robinson M.A., Gallagher D.L., Reay W.G., 1998. Field observations of tidal and seasonal variations in ground water discharge to estuarine surface waters. Ground Water Monitoring and Remediation. 18 (1): 83-92.

Shen Z., Zhu Y., Zhong Z., 1993. Theoretical basis of hydrogeochemistry. Geological Publishing House. Beijing, China. (in Chinese)

Sherif M.M., Singh V.P., 1999. Effect of climate change on sea water intrusion in coastal aquifers. Hydrological Processes 13, 8:1277-1287.

Shi M.Q., 2012. Spatial distribution of population in the low elevation coastal zone and assessment on vulnerability of natural disaster in the coastal area of China. Master thesis of Shanghai Normal University, 24–32.(Chinese with English abstract)

Simpson, M.J., Clement, T.P., 2004. Improving the worthiness of the Henry problem as a benchmark for density-dependent groundwater flow models. Water Resources Research 40 (1), W01504 doi:10.1029/2003WR002199.

Sivan O., Yechieli Y., Herut B., Lazar B., 2005. Geochemical evolution and timescale of seawater intrusion into the coastal aquifer of Israel. Geochimica et Cosmochimica Acta. 69(3):579-592.

Smith A.J., Turner J.V., 2001. Density-dependent surface water-groundwater interaction and nutrient discharge in the Swan-Canning Estuary. Hydrolological Processes. 15:2595-2616.

SOA (State Oceanic Administration of the People's Republic of China), 2015. China's Marine Environment Bulletin: 2014. Released 11th March, (in Chinese).

Sophocleus M., 2002. Interactions between groundwater and surface water: the state of science.

Hydrol. Earth Syst. Sci. Discuss., https://doi.org/10.5194/hess-2017-617
Manuscript under review for journal Hydrol. Earth Syst. Sci.
Discussion started: 7 November 2017

Hydrogeology Journal. 10:52-67.

Sun J., Yang Y., 2007. Seawater intrusion characteristics in Qinhuangdao. Journal of Environmental Management College of China. 17(2):51-54. (Chinese with English abstract)

UN Atlas, 2010. UN Atlas: 44 Percent of us Live in Coastal Areas. <http://coastalchallenges.com/2010/01/31/un-atlas-60-of-us-live-in-the-coastal-areas/>.

Vengosh A., Gill J., Reyes A., Thoresberg K., 1997. A multi-isotope investigation of the origin of ground water salinity in Salinas Valley, California. American Geophysical Union, San Francisco, California.

Vengosh A., Pankratov I., 1998. Chloride/bromide and chloride/fluoride ratios of domestic sewage effluents and associated contaminated ground water. Ground Waer. 36(5):815-824.

Wang J., Yao P., Bianchi T.S., Li D., Zhao B., Cui X., Pan H., Zhang T., Yu Z., 2015. The effect of particle density on the sources, distribution, and degradation of sedimentary organic carbon in the Changjiang Estuary and adjacent shelf. Chemical Geology. 402:52-67.

Werner A.D., 2010. A review of seawater intrusion and its management in Australia. Hydrogeology Journal. 18(1):281-285.

Werner A.D., Bakker M., Post V.E.A., Vandenbohede A., Lu C., Ataie-Ashtiani B., Simmons C.T., Barry D.A., 2013a. Seawater intrusion processes, investigation and management: Recent advances and future challenges. Advances in Water Resources.51:3-26.

Werner A.D., Simmons C.T., 2009. Impact of sea-level rise on seawater intrusion in coastal aquifers. Ground Water. 47:197-204.

Westbrook S.J., Rayner J.L., Davis G.B., Clement T.P., Bjerg P.L., Fisher S.J., 2005. Interaction between shallow groundwater, saline surface water and contaminant discharge at a seasonally and tidally forced estuarine boundary. Journal of Hydrology, 302:255-269.

Wilhite D.A., 1993.Drought Assessment, Management, and Planning: Theory and Case Studies. Springer U S. p628.

Xu G., 1986. Analysis of seawater intruding into aquifer system in Beidaihe Region.Hydrogeology & Engineering Geology. 2:7-10. (in Chinese)

Xue Y., Wu J., Xie C., Zhang Y., 1997. Study of seawater and saltwater intrusion in the coast plain of Laizhou Bay. Chinese Science Bulletin. 42(22):2360-2367. (in Chinese)

Xue Y.Q., Wu J.C., Ye S.J., Zhang Y.X., 2000. Hydrogeological and hydrogeochemical studies for salt water intrusion on the South Coast of Laizhou Bay, China. Ground Water. 38, 38-45.

Yang H., 1996. Sea-level changes in east China over the past 20000 years. in Study of Environmental Change. Hohai University Press. Nanjing, China. pp390-395.

Yang L., 2011. Formation mechanism of bedrock fracture type-geothermal water in Qinhuangdao area. West-china Exploration Engineering. Urumchi, China. 10:151-152. (in Chinese)

Yang Y., Gao S., Xie Y., 2008. Assessment and control countermeasures of seawater intrusion hazard on Qinhuangdao Region. The Chinese Journal of Geological Hazard and Control. 19(3):139-143. (Chinese with English abstract)

Yang Y., He Q., Xie Y., Cao C., 1994. Grey model prediction of seawater intrusion of Qinhuangdao. The Chinese Journal of Geological Hazard and Control. 5(sup.):181-183. (Chinese with English abstract)

Yechieli Y., Kafri U., Sivan O., 2009. The inter-relationship between coastal sub-aquifers and the Mediterranean Sea, deduced from radioactive isotopes analysis. Hydrogeology Journal. 17:265-274.

Zang W., Liu W., Guo J., Zhang X., 2010. Geological hazards of seawater intrusion and its control measures in Qinhuangdao City, Hebei Province. The Chinese Journal of Geological Hazard and Control. 21(4):120-125. (Chinese with English abstract)

Zeng J., 1991. Geochemistry of geothermal water in Qinhuangdao area, Hebei Province. Bull. Institute of Hydrogeology and Engineering Geology, Chinese Academy of Geological Sciences. 7:111-127.

Zhang B., 2012. Mechanism of Seawater Intrusion Using Hydrochemistry and Environmental Isotopes in Qinhuangdao Yang Dai River Plain. Master's Thesis. Xiamen University, Fujian, China. (Chinese with English abstract)

Zhang Q., Volker R.E., Lockington D.A., 2004. Numerical investigation of seawater intrusion at Gooburrum, Bundaberg, Queensland, Australia. Hydrogeol. J. 12 (6), 674-687.

Zhang Z., Peng L., 1998. Groundwater hydrochemical characteristics on seawater intrusion in eastern and southern coasts of Laizhou Bay. China Environmental Science. 18(2):121-125.

Zhuang Z., Liu D., Yang M., Li H., Qiu H., Ning P., Song W., Xu Z., 1999. The role of anthropogenic activities in the evolution of saline water intrusion processes. Journal of Ocean University of Qingdao. 29(1):141-147. (Chinese with English abstract)

Zuo W., 2006. Survey and Research on Seawater Intrusion in the Yandaihe Plain of Qinhuangdao City. Doctoral Thesis. China University of Geosciences, Beijing, China. (Chinese with English abstract)

Zuo W., Yang Y., Dong Y., Liang M., 2009. The numerical study for seawater intrusion in Yanghe and Daihe coastal plain of Qinhuangdao City. Journal of Natural Resources. 24(12):2087-2095. (Chinese with English abstract)

Hydrol. Earth Syst. Sci. Discuss., https://doi.org/10.5194/hess-2017-617
Manuscript under review for journal Hydrol. Earth Syst. Sci.
Discussion started: 7 November 2017

Hydrology and Earth System Sciences
Open Access
Discussions

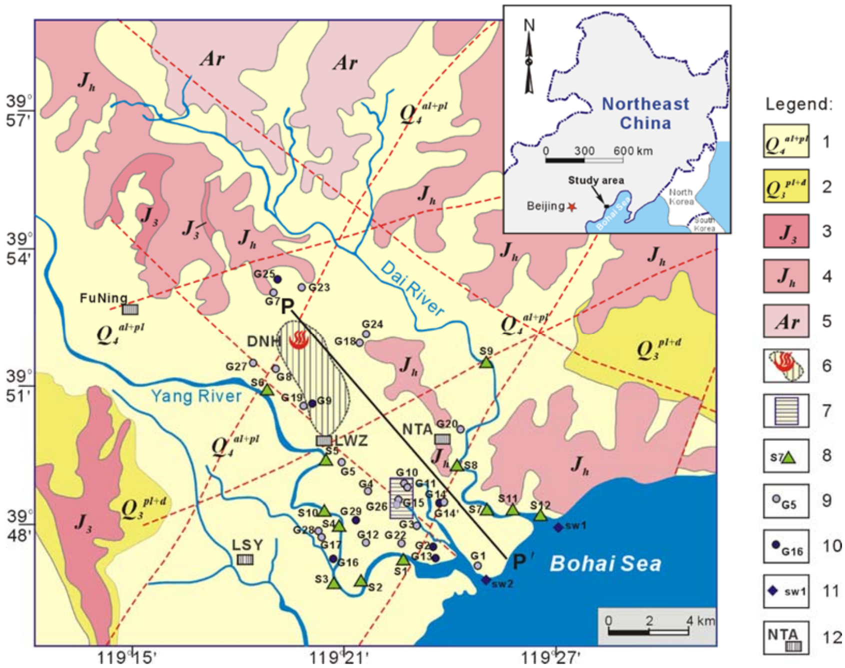

Figure 1. Map for showing geological background and water sampling sites in the study area
Explanation for the legend: 1-Holocene (al- alluvial, pl- pluvial) sediments; 2- Upper Pleistocene (dpl-proluvial-deluvial) sediments; 3- Jurassic andesite; 4- Jurassic migmatitic granite; 5- Archaean group gneiss; 6-Geothermal field location and its influence area; 7- Zaoyuan well field; 8- surface water sampling site; 9-shallow groundwater sampling site; 10- deep groundwater sampling site; 11- seawater sampling site; 12-village/county site (DNH-Danihe; NTA-Niutouai; LWZ-Luwangzhuang; LSY-Liushouying). The red dashed lines are showing the buried fault distribution in this area.

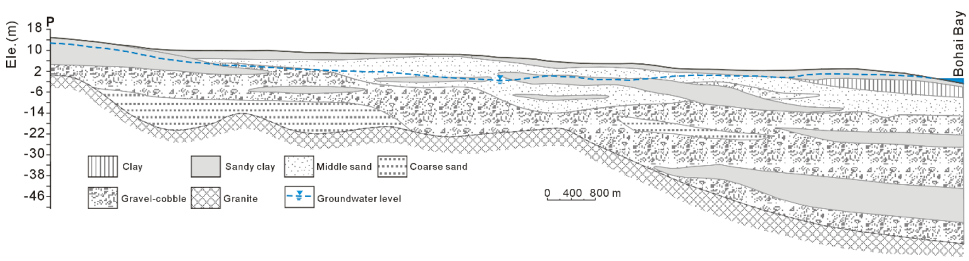

Figure 2. Hydrogeological cross-section of Yang-Dai River Plain (P-P′ in Fig. 1) (modified from Han, 1988)

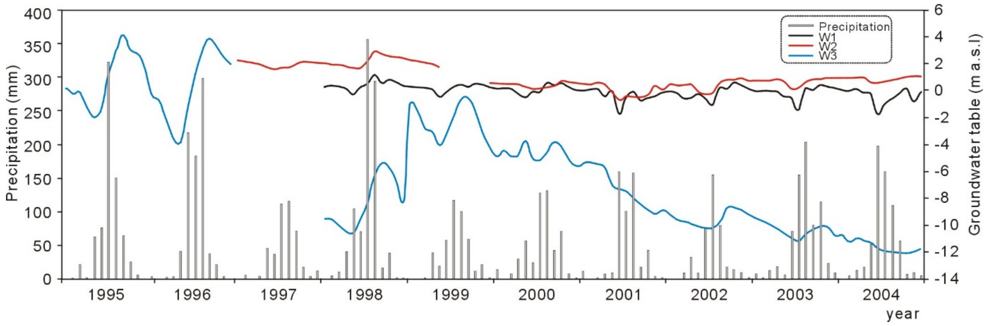

Figure 3. Distribution of precipitation and dynamics of groundwater table in the study area

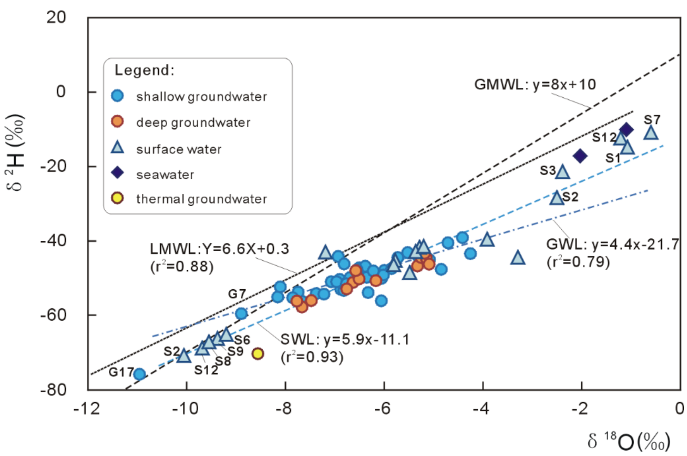

Figure 4. Stable isotope compositions of different water samples collected from the study area
LMWL - local meteoric water line; GMWL – global meteoric water line (Craig, 1961); GWL – groundwater line; SWL – surface (river) water line.

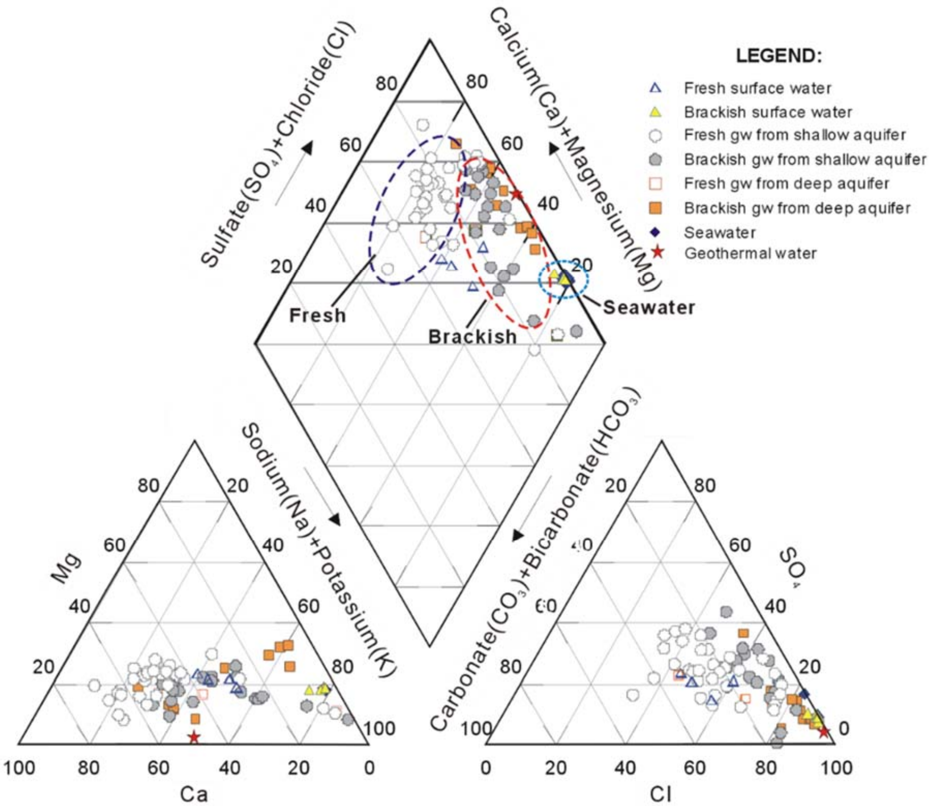

Figure 5. Piper plot of different water samples

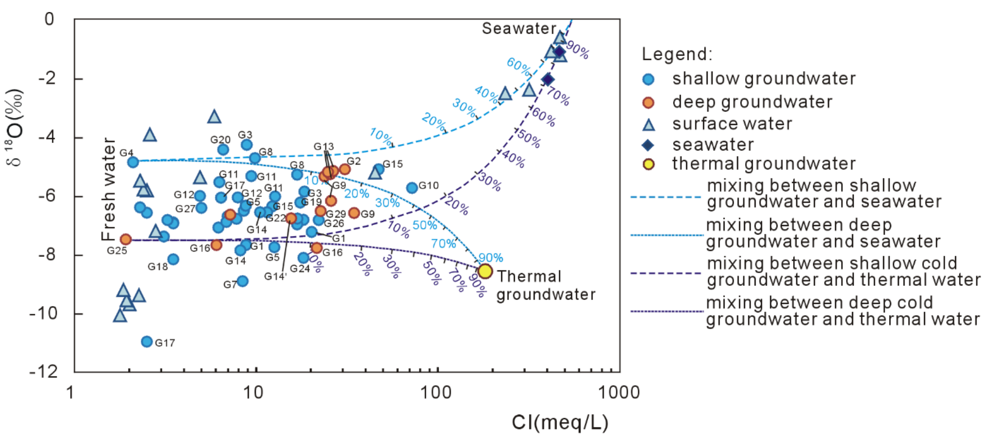

Figure 6. Relationship between chloride content and isotopic signature of different water samples as a means to differentiate mixing processes in the area. The data of thermal water are from Zeng (1991).

Hydrology and Earth System Sciences
Open Access
EGU
Discussions

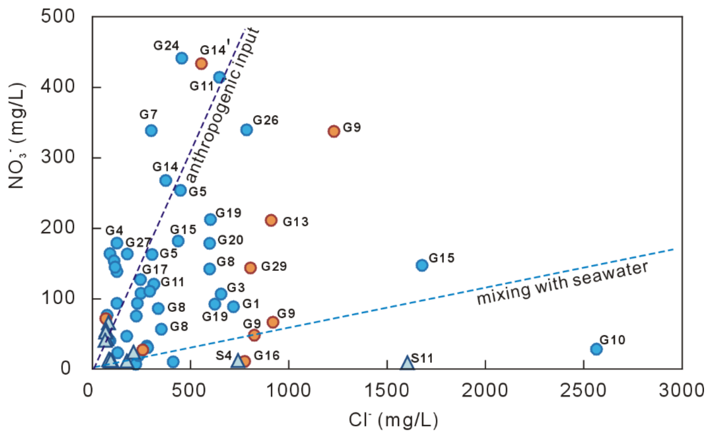

Figure 7. Plots of chloride versus nitrate concentrations. Symbols are same as in Fig. 6.

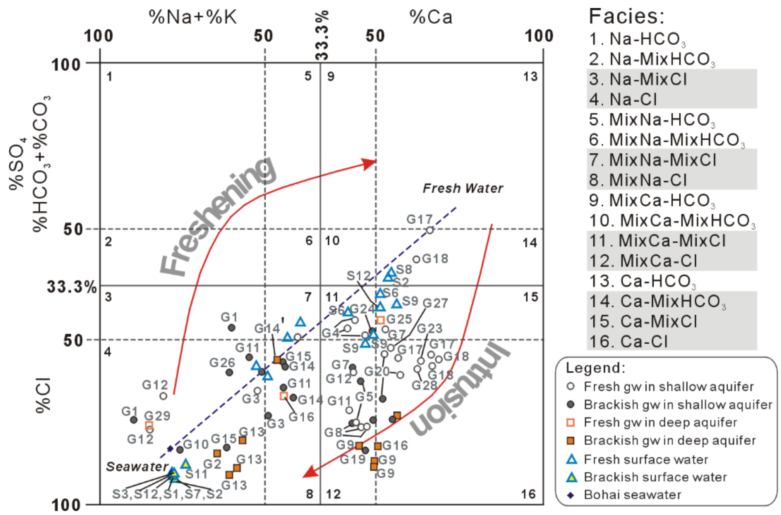

Figure 8. Hydrogeochemical facies evolution diagram (HFE-D) for the collected water samples

Hydrology and Earth System Sciences
Discussions
Open Access

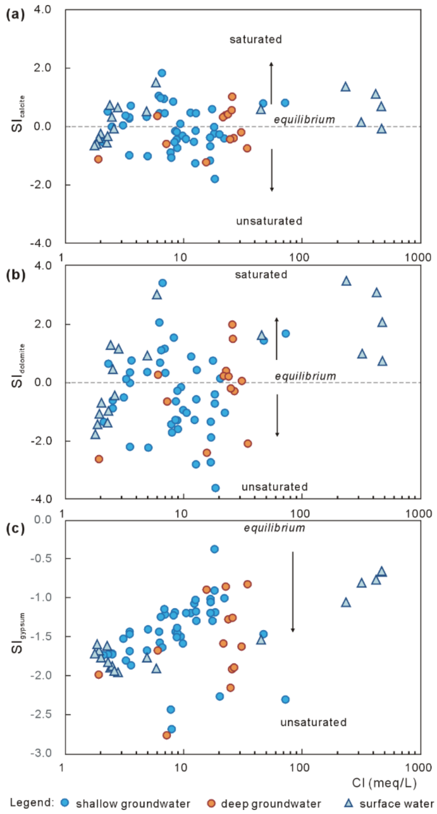

Figure 9. Variation of saturation indices with respects to calcite (a), dolomite (b) and gypsum (c) versus chloride concentrations

Hydrol. Earth Syst. Sci. Discuss., https://doi.org/10.5194/hess-2017-617
Manuscript under review for journal Hydrol. Earth Syst. Sci.
Discussion started: 7 November 2017

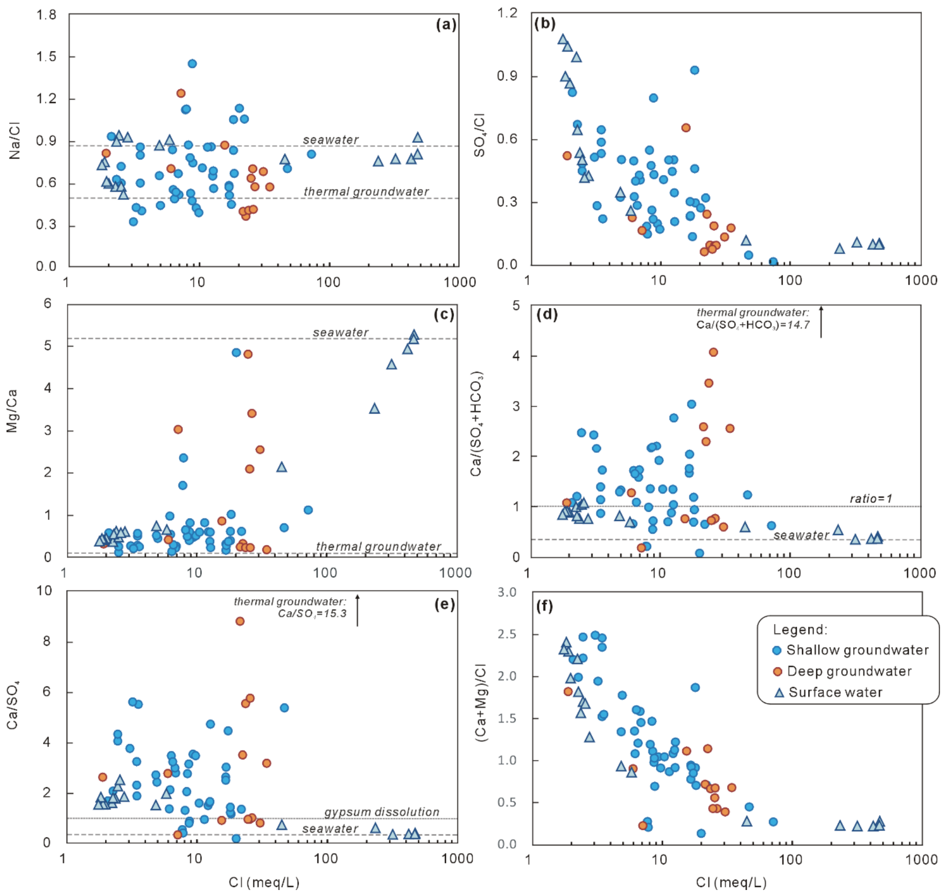

Figure 10. Molar ratios of major ions versus chloride concentrations for different water samples from the study area

Hydrol. Earth Syst. Sci. Discuss., https://doi.org/10.5194/hess-2017-617
Manuscript under review for journal Hydrol. Earth Syst. Sci.
Discussion started: 7 November 2017

Hydrology and Earth System Sciences
Open Access
Discussions

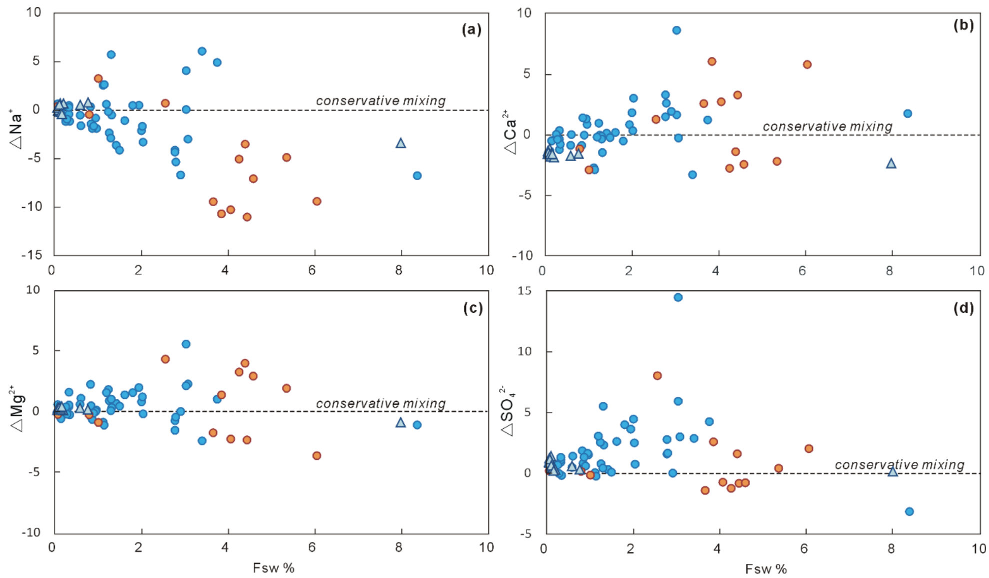

Figure 11. ΔNa^{+} (a), ΔCa^{2+} (b), ΔMg^{2+} (c) and ΔSO_4^{2-} (d) versus calculated seawater percentage (F_{sw}%)

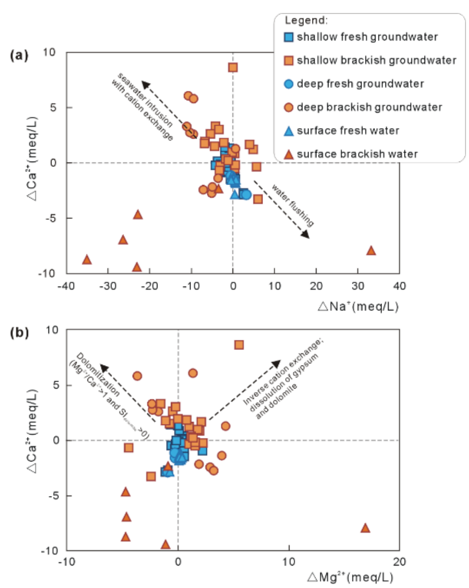

Figure 12. Distribution of cationic deltas (a)- ΔNa^{+} versus ΔCa^{2+}; (b) ΔMg^{2+} versus ΔCa^{2+} for each sample (in meq/L)

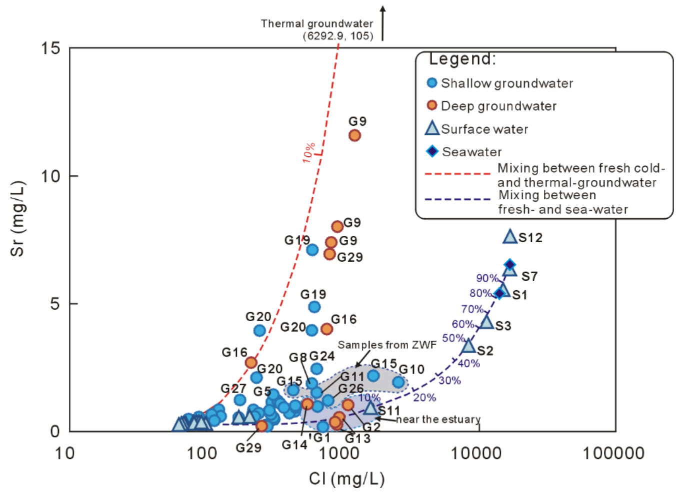

Figure 13. Chloride versus strontium concentrations of different water samples

ZWF- Zaoyuan well field

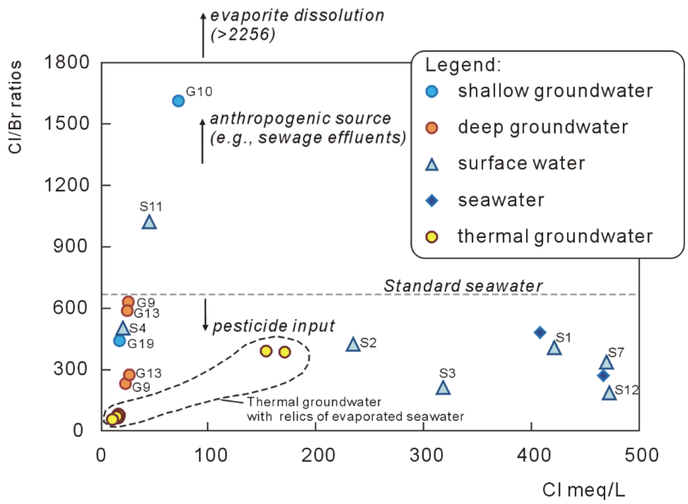

Figure 14. Chloride versus bromide to chloride molar ratios. Data of 8 thermal groundwater samples are from Zeng (1991) and Hui (2002).

Hydrol. Earth Syst. Sci. Discuss., https://doi.org/10.5194/hess-2017-617
Manuscript under review for journal Hydrol. Earth Syst. Sci.
Discussion started: 7 November 2017

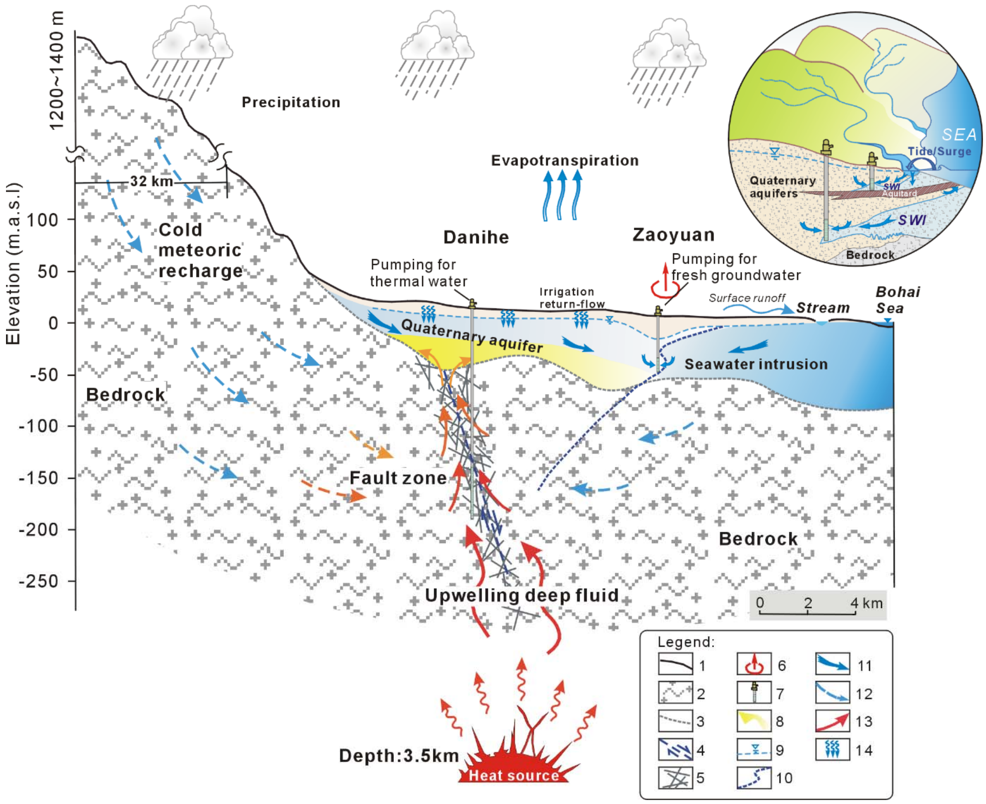

Figure 15. Conceptual model of groundwater flow system in the Yang-Dai River coastal plain

Explanation: 1- Land surface; 2- Bedrock; 3- Boundary between Quaternary sediments and bedrock; 4-Fault; 5- Permeable fracture zone; 6- Concentrated groundwater pumping zone; 7- Pumping wells; 8- Zone affected by upflow of geothermal fluids; 9- Groundwater table; 10- Potential interface between fresh- and salt-water; 11-Groundwater flow direction in Quaternary aquifers; 12- Groundwater flow in bedrocks; 13- Geothermal groundwater flow direction; 14- Irrigation return-flow.

Hydrol. Earth Syst. Sci. Discuss., https://doi.org/10.5194/hess-2017-617
Manuscript under review for journal Hydrol. Earth Syst. Sci.
Discussion started: 7 November 2017

Hydrology and Earth System Sciences
Open Access
Discussions

Table 1. Physical, hydrochemical and isotopic data of the water samples collected from the Yang-Dai River coastal plain

WaterType	ID	Sampling Time	Ele.	WellDepth	WaterTable Depth(m)	EC	pH	T	ORP	DO	Cl^-	NO_3^-	SO_4^{2-}	HCO_3^-	Ca^{2+}	Na^+	K^+	Mg^{2+}	Sr	δ^2H	$\delta^{18}O$
			m	m		μs/cm		ºC	mV	mg/L	mg/L	mg/L	mg/L	mg/L	mg/L	mg/L	mg/L	mg/L	mg/L	‰	‰
Shallow groundwater samples:																					
Fresh Groundwater	G4	Aug.2010	5	15	4.2	741	6.5	20.5	6	3.9	124.3	92.6	89.7	136.9	70.3	69.2	2.3	21.8	0.67	-50	-6.9
	G27	Aug.2010	3	12		1014	6.4	14.8	16	3.8	177.5	163.0	121.0	128.0	122.0	50.6	2.6	33.4	1.22	-50	-6.4
	G12	Aug.2010	8	10		1152	7.2	25.0	9	5.9	276.9	31.9	69.8	148.8	15.8	201.9	11.1	16.2	0.25	-51	-6.8
	G17	Aug.2010	5	25	5.7	624	7.1	19.1	13	3.3	88.8	39.5	58.3	223.3	98.4	41.4	4.3	7.5	0.33	-76	-11.0
	G18	Aug.2010	5	23	1.7	934	7.4	14.9	12	7.1	124.3	137.8	98.7	235.2	133.3	48.3	2.2	23.2	0.71	-55	-8.2
	G1	Sep.2009	6	8	2.4	1673	8.3	19.4			220.1	2.0	148.3	207.9	84.3	119.6	17.1	49.9	0.66	-51	-7.1
	G4	Sep.2009	6	15	4.6	1295	7.9	13.9			124.3	178.5	108.7	92.4	104.4	64.4	2.7	35.9	0.85	-44	-6.9
	G5	Sep.2009	11	16	6.5	1544	7.8	13.3			303.4	162.3	108.2	38.5	124.5	103.7	1.1	39.1	1.14	-47	-6.5
	G23	Sep.2009	15	30	3.0	556	7.9	14.9			88.8	163.4	54.0	51.9	97.4	34.5	0.5	15.6	0.55	-48	-6.6
	G7	Sep.2009	17	8	1.7	901	8.4	14.9			81.7	41.2	74.2	69.3	64.0	33.2	1.0	16.5	0.41	-47	-6.4
	G8	Sep.2009	4	13	4.3	1621	7.8	14.0			334.6	85.4	90.1	69.3	132.5	91.9	1.4	38.5	1.19	-44	-5.3
	G11	Sep.2009	4	13		1237	8.6	18.4			222.9	74.5	98.7	30.8	87.4	80.1	1.8	29.0	0.84	-43	-5.5
	G12	Sep.2009	8	10		1114	7.9	15.0			174.0	46.0	76.4	107.8	86.2	73.6	4.3	27.2	0.53	-48	-6.0
	G28	Sep.2009	6	23	6.8	1748	8.2	14.6			127.8	22.5	38.4	107.8	88.2	33.3	1.3	14.0	0.58		
	G18	Sep.2009	9	23	5.5	2850	7.8	13.7			110.1	152.9	76.7	53.9	120.3	23.1	1.1	20.5	0.65	-54	-7.4
	G20	Sep.2009	12	30		1602	7.7	19.5			246.9	107.1	135.9	107.8	158.2	82.8	1.7	26.3	3.94	-50	-6.7
	G17	Sep.2009	6	33	7.9	819	8.1	14.3			243.5	126.4	141.7	161.7	176.3	105.5	1.8	24.6	0.71	-53	-6.9
	G3	Jun.2008	4	20		1573	7.3	14.5			315.0		184.4	54.9	67.3	152.1	3.8	33.2	0.46	-43	-4.2
	G4	Jun.2008	6	6		688	7.5	14.1			74.6	75.8	83.2	60.4	58.2	45.2	1.2	20.6	0.47	-48	-4.8
	G5	Jun.2008	5	11		1455	7.4	14.7			310.9	119.5	92.7	52.2	121.3	95.4	0.9	29.9	1.43	-54	-6.3
	G8	Jun.2008	4	30		1402	7.3	14.7			349.7	55.9	81.5	85.1	118.0	88.1	1.2	36.9	1.08	-40	-4.7
	G12	Jun.2008	8	10		1285	7.6	19.3			281.0	29.8	56.8	74.1	9.7	205.7	11.0	13.7	0.19	-50	-6.0
	G17	Jun.2008	6	33		1462	8.1	15.0			227.9	92.6	123.8	175.7	179.2	72.1	1.1	15.9	0.57	-56	-6.1
	G18	Jun.2008	9	23		1125	7.9	18.8			115.5	144.2	44.4	90.6	103.7	31.8	1.4	13.7	0.41	-53	-6.8
	G20	Jun.2008	12	30		1210	9.1	28.3			234.3	18.2	90.6	230.6	122.0	81.4	2.6	22.4	2.10	-39	-4.4
Brackish Groundwater	G1	Aug.2010	6	11		2750	7.4	17.3	143	1.5	312.4	120.0	337.1	205.4	112.0	294.4	29.9	41.3	0.54	-56	-7.7
	G3	Aug.2010	4	8		2490	5.9	14.7	74	1.4	654.3	106.0	263.7	86.3	128.2	283.6	6.6	78.6	0.97	-47	-5.8
	G15	Aug.2010	4	30		2290	6.6	15.4	3	3.3	435.7	181.3	263.7	244.1	164.3	242.8	6.6	60.8	1.60	-50	-6.3
	G26	Aug.2010	4	18	1.8	4060	6.4	15.2	145	1.3	784.6	339.4	341.4	485.2	192.3	538.2	36.0	72.1	1.20	-46	-6.8
	G11	Aug.2010	6	13	2.3	3490	6.5	15.0	47	1.3	646.1	414.1	402.7	402.6	204.8	441.8	34.9	76.3	1.51	-52	-6.8
	G20	Aug.2010	12	30		1513	6.7	18.8	4	4.3	596.4	177.9	245.0	184.6	268.6	225.4	2.0	29.2	3.95	-51	-7.0
	G5	Aug.2010	5	16	5.4	1500	6.2	15.6	7	5.9	447.3	253.3	304.7	79.3	204.1	188.6	0.8	47.5	0.78	-54	-7.7
	G8	Aug.2010	4	30	2.1	1563	6.3	15.7	120	4.9	596.4	141.4	188.1	104.2	196.3	220.8	3.2	38.7	1.87	-44	-5.3
	G7	Aug.2010	5	8	0.9	1438	6.8	19.3	24	6.1	299.6	338.3	192.7	128.0	164.2	151.8	0.3	50.0	0.66	-60	-8.9
	G19	Aug.2010	8	11	2.8	2380	6.5	16.1	42	3.2	600.0	211.9	192.1	119.1	241.4	199.5	6.6	42.4	7.10	-52	-6.8
	G24	Aug.2010	4	21		4400	6.8	15.5	4	5.9	646.1	952.1	813.3	223.3	484.1	349.6	3.4	117.4	2.44	-52	-8.1
	G22	Sep.2009	2	20	2.0	2170	8.0	17.8			408.3	2.0	277.5	130.9	109.2	226.8	21.3	54.2	0.70	-48	-6.5
	G10	Sep.2009	3	18		9770	7.5	15.1			2563.1	27.7	25.3	870.2	181.4	1340.0	98.1	123.0	1.92	-44	-5.7
	G14	Sep.2009	2	8.5		1886	8.5	16.6			291.1	109.8	216.4	92.4	117.8	164.7	19.3	46.5	0.82	-55	-7.9

	G24	Sep.2009	11	21	5.3	1003	7.8	13.6			454.4	441.5	128.1	115.5	252.3	165.6	0.6	36.2	0.93		
	G19	Sep.2009	12	11	4.7	2560	8.1	14.6			622.0	91.5	115.6	69.3	214.9	180.7	6.0	49.4	4.87	-48	-6.2
	G1	Jun.2008	6	8		3150	8.5	15.0			717.1	87.7	265.6	98.8	9.1	527.4	26.7	26.6	0.17	-54	-7.2
	G11	Jun.2008	6	13		2370	7.2	12.2			451.2		211.3	162.0	145.1	201.2	22.0	52.6	1.00	-49	-6.0
	G14	Jun.2008	3	8.5		2050	7.4	18.6			372.8	267.3	206.1	49.4	136.4	171.3	12.7	49.5	0.93	-48	-6.5
	G15	Jun.2008	4	18		5990	7.5	15.6			1675.6	146.8	110.1	474.9	246.5	764.7	20.2	104.9	2.17	-45	-5.1
Deep Groundwater samples:																					
Fresh Groundwater	G25	Aug.2010	4	95		444	6.6	23.5	41	4.4	68.1	71.0	48.2	89.3	52.5	35.9	1.1	10.4	0.25	-56	-7.5
	G16	Sep.2009	3	110		1214	7.9	19.9			214.4		66.1	100.1	76.3	97.8	2.8	19.5	2.68	-58	-7.7
	G29	Sep.2009	6	60		1291	8.1	20.9			255.6	26.3	57.5	69.3	8.0	205.9	12.3	14.6	0.20	-51	-6.6
Brackish Groundwater	G29	Aug.2010	6	60	6.2	3220	7.2	24.1	12	5.6	803.4	143.0	264.7	178.6	386.8	189.3	4.3	77.6	6.95	-50	-6.5
	G16	Aug.2010	3	110		1733	7.3	21.5	16	4.8	766.8	5.5	67.1	205.4	246.2	197.8	4.5	37.9	4.00	-56	-7.8
	G9	Jun.2008	9	104		3110	7.8	15.0			823.6	47.4	110.5	85.1	255.1	222.2	5.1	36.7	7.40	-47	-5.3
	G9	Sep.2009	9	104		3190	8.5	20.4			917.4	65.8	116.6	61.6	279.8	245.1	5.7	40.6	8.02	-51	-6.2
	G9	Aug.2010	9	104		4600	6.3	24.3	18	4.0	1228.3	337.4	296.3	92.3	392.2	455.4	5.5	45.3	11.59	-48	-6.6
	G14'	Aug.2010	5	110	2.1	2850	6.1	22.9	120	1.8	553.8	433.7	491.4	134.0	186.0	312.8	52.3	96.6	1.06	-53	-6.8
	G13	Aug.2010	3	90		3230	8.9	19.2	36	2.4	908.8	210.6	231.8	92.3	92.0	413.5	29.0	115.7	0.26	-45	-5.2
	G13	Jun.2008	3	90		3180	7.9	13.5			945.4		122.2	52.2	51.4	351.9	25.0	105.4	0.55	-45	-5.1
	G13	Sep.2009	3	90	2.6	3070	8.1	15.3			882.0		91.9	38.5	36.5	362.9	26.0	105.3	0.35	-43	-5.2
	G2	Jun.2008	2	60		3780	7.7	18.5			1093.4		200.3	96.1	67.3	484.1	25.8	103.1	1.03	-46	-5.1
River water samples:																					
Fresh water samples																					
Dai River	S9	Aug.2010				511	7.2	22.2	22	5.5	80.3	65.2	107.9	86.3	72.1	29.9	3.7	16.7	0.34	-66	-9.4
Dai River	S12	Aug.2010				485	7.5	25.8	18	7.3	71.3	41.9	83.7	83.4	54.3	27.6	4.0	15.1	0.30	-69	-9.7
Dai River	S8	Aug.2010				495	7.3	22.1	24	5.8	68.6	54.9	96.8	89.3	62.3	27.2	4.1	15.9	0.32	-67	-9.6
Yang River	S6	Aug.2010				507	7.0	23.3	17	4.5	66.0	51.9	80.5	107.2	61.6	32.2	3.8	16.8	0.30	-65	-9.2
Yang River	S2	Aug.2010				435	7.3	7.3	6	4.9	63.2	40.2	92.2	101.2	59.3	29.9	4.3	14.0	0.26	-71	-10.1
Yang River	S5	Sep.2009				718	8.4	24.4			85.2	12.9	62.0	107.8	46.1	52.0	6.4	17.4	0.36	-45	-5.8
Yang River	S4	Sep.2009				2630	8.1	24.7			733.1	6.6	142.2	115.5						-42	-5.3
Yang River	S6	Sep.2009				718	8.3	25.6			99.4	6.6	57.5	107.8	44.3	59.8	5.0	16.4	0.30	-43	-7.2
Dai River	S9	Sep.2009			2.0	560	8.0	23.6			88.8	6.8	60.5	92.4	57.2	33.2	3.3	16.7	0.36	-46	-5.8
Dai River	S8	Sep.2009				1013	8.2	23.6			174.0	6.4	82.2	92.4	52.1	98.1	6.0	23.6	0.55	-43	-5.4
Yang River	S6	Jun.2008				1166	7.5	12.6			81.7	12.6	71.3	112.5	53.6	47.5	4.9	18.0	0.31	-49	-5.5
Dai River	S10	Jun.2008				1255	9.1	28.0			208.9	23.1	73.7	175.7	60.7	123.2	10.8	24.2	0.57	-44	-3.3
Dai River	S9	Jun.2008				1163	7.8	11.8			92.3	7.5	52.2	90.6	54.7	31.1	3.6	19.5	0.35	-40	-3.9
Brackish and salt water samples																					
Yang River	S3	Sep.2009				34800	7.8	15.5			11289.4		1684.7	115.5	251.0	5658.7	231.3	690.1	4.29	-21	-2.4
Dai River	S12	Sep.2009				47100	7.5	23.7			16766.3		2416.5	77.0	412.1	10074.3	398.2	1306.0	7.64	-12	-1.2
Dai River	S11	Sep.2009				52500	8.5	23.4			1601.5	2.8	258.7	84.7	79.7	801.4	32.9	102.7	0.93	-41	-5.2
Yang River	S1	Jun.2008				39800	8.7	24.2			14953.5		2035.9	134.5	313.0	7496.0	270.5	928.3	5.55	-15	-1.1
Yang River	S2	Jun.2008				20200	8.8	28.5			8328.3		912.1	189.4	233.4	4094.2	147.9	495.9	3.37	-28	-2.5
Dai River	S7	Jun.2008				49500	8.4	11.5			16677.1		2261.3	113.9	349.0	8730.0	326.4	1084.0	6.36	-11	-0.6
	SW1	Aug.2010				45600	7.8	25.5	83	4.90	14768.3	810.1	4047.0	148.8	312.7	8326.4	293.6	1007.0	5.79	3.8	1.1
Seawater:	SW1	Sep.2009				47700	7.8	24.2			16568.0		2394.3	92.4	352.2	8922.0	322.2	1107.0	6.45	-10	-1.1
	SW2	Sep.2009				39500	7.3	23.2			14484.8		1926.6	107.8	313.2	7214.0	267.9	916.9	5.43	-17	-2.0